An evaluation of the basin architecture and dynamics during the deposition of the Zechstein, Late Permian

Graduate Internship at EBN B.V.

E. A. Wijnen

e.a.wijnen@students.uu.nl

External supervisor: Kees van Ojik

Internal supervisor: Dr. Paul Meijer

Department of Earth Sciences, Faculty of Geosciences, Utrecht University

20 May 2022

30 ECTS

Abstract

In this report a quantitative analysis of the Zechstein deposits is presented. The Zechstein was deposited during the Late Permian in the Southern Permian Basin (SPB), an intercratonic basin that reached from the UK to Latvia. The Zechstein consist of seven cycles, of which five cycles are present in the subsurface of the Netherlands. They are referred to as the Z1-Z5 and consist of a somewhat fixed pattern of deposits: from base to top a claystone, followed by carbonates, anhydrites and halites (and ultimately magnesium-potassium salts). Some variation in distribution and thickness between the different cycles can be observed. The cyclicity in the Zechstein has been attributed to difference in water levels due to Gondwana glaciation cycles, in combination with high evaporation rates. Furthermore, the Zechstein is believed to have been formed in the shallow water-deep basin setting. The goal of this internship is to improve our understanding of the basin architecture and dynamics of the SPB during the deposition of the Zechstein and more specifically, to further apprehend the causes for the cyclicity, the variations in thickness and distribution of the Zechstein sediments and the type of basin in which the Zechstein has been deposited. The volumes of the different lithologies have been established using distribution and thickness maps in combination with well tops from the offshore Netherlands. Using the concentration of the minerals in Permian seawater necessary for deposition of these lithologies and their saturation concentrations, the volumes of seawater required for the deposition of Zechstein carbonates, gypsums and halites have been determined, as well as the duration of deposition of these sediments. A cross-section through the Z1 in the offshore Netherlands was afterwards constructed to assess the accommodation space in the basin, and by compensating for the vertical response as predicted by the isostatic balance the basin architecture and dynamics can be investigated. The total volume of the Zechstein cycles is mainly controlled by the halites, which have the largest volumes of all the different types of lithologies. The Z2 halite (and thus the Z2 cycle) is the largest and decreases with each following cycle. The seawater volume necessary for the deposition of the carbonate is the most significant, with an average water column of 400 km for the Z2 carbonate. The gypsum deposits require significantly less water and the halite deposits requires the least amount of water. The calculated total duration of deposition lies between 285 kyr and 1.04 Myr, in which the halite series are deposited in the shortest timeframe. It can be concluded that there must have been a constant connection to a marine source during the deposition of the carbonates and the gypsums, as well as a water-flux out of the basin. Both are not necessary during the deposition of the halite. The cyclicity within the Zechstein deposits can be explained by variations in the isostatic balance, to which the delayed isostatic subsidence of the halite contributes significantly. The shallower water-shallow basin model seems to best explain the basin in which the Zechstein was deposited. This analysis is however based on several assumptions and uncertainties, and the construction of a more realistic 3D model would be most effective to further investigate the basin dynamics during the deposition Zechstein.

Contents

1 Introduction

In this report a quantitative analysis of the Zechstein deposits is presented. The Zechstein deposits are present in the subsurface of the Netherlands, in which both natural gas and oil have been discovered and which acts a seal for the Upper Rotliegend reservoir (De Jager et al., 2007). Within the Zechstein deposits a certain cyclicity can be found, which has been contributed to difference in water levels due to glaciations (Van der Baan, 1990; Peryt et al., 2010). However, the question may arise whether this is the most obvious explanation and if there are other possibilities that explain this.

The goal of this internship is to improve our understanding of the basin architecture and dynamics of the Southern Permian Basin during the deposition of the Zechstein and more specifically, to further apprehend the causes for the cyclicity and the variations in thickness and distribution of the Zechstein sediments. In order investigate this, the volumes of the different lithologies of the Zechstein and the volumes of water necessary for deposition of these lithologies have been determined. This information can be used to assess the accommodation space in the basin and by compensating for the vertical response as predicted by the isostatic balance, as described by Van den Belt & de Boer (2007), the basin architecture and dynamics can be investigated.

There are three types of basin-models that could explain the formation of the Zechstein. These basin-models can be found in Figure 1.1: the deeper water-deep basin, the shallower water-deep basin and the shallower water-shallow basin model. The types of deposits found in these models are in generally based on the depth of water in the basin (although it is unclear what exactly deep and what exactly shallow water is). In the deeper water-deep basin model the basin is hydrologically isolated from the ocean and

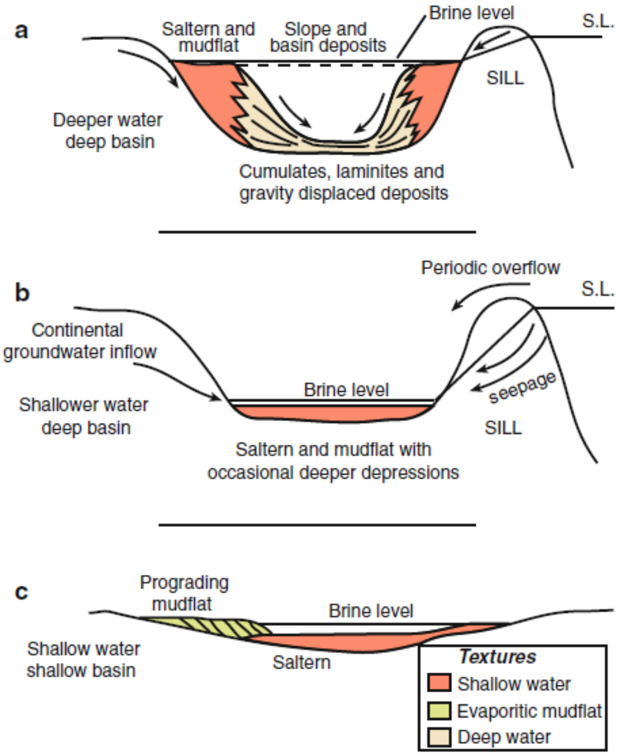

Figure 1.1. The three different types of basin-models, from Warren (2016).

receives water from seepage from a marine source. The water level in the shallower water-deep basin model is located substantially under the sea level and receives water from periodic overflow, seepage and continental groundwater. The shallow water-shallow basin has an open connection to a marine source (Warren, 2016). The Zechstein is believed to have been formed in the shallow water-deep basin model (Van den Belt & de Boer, 2007).

1.1 Geological setting

The Zechstein deposits were deposited in the Late Permian in the Southern Permian Basin (SPB). This is an intercratonic basin, formed after the Variscan Orogeny, that spreads from the UK to Latvia (Peryt et al., 2010). The paleogeography of the SPB during the deposition of the second Zechstein cycle (the Z2) is illustrated in Figure 1.2. The SPB was located at a paleolatitude of ~20° N and arid conditions were prevailing during the deposition of the Zechstein (Geluk, 2005; Legler et al., 2005).

The SPB formed due to thermal relaxation of the crust due to the collapse of the Variscan orogen (Van der Baan, 1990; Van Wees et al., 2000; Peryt et al., 2010). The cyclicity of the deposits is believed to be caused by a combination of high evaporation rates and eustatic sea-level changes due to Gondwana glaciation cycles (Van der Baan, 1990; Peryt et al., 2010).

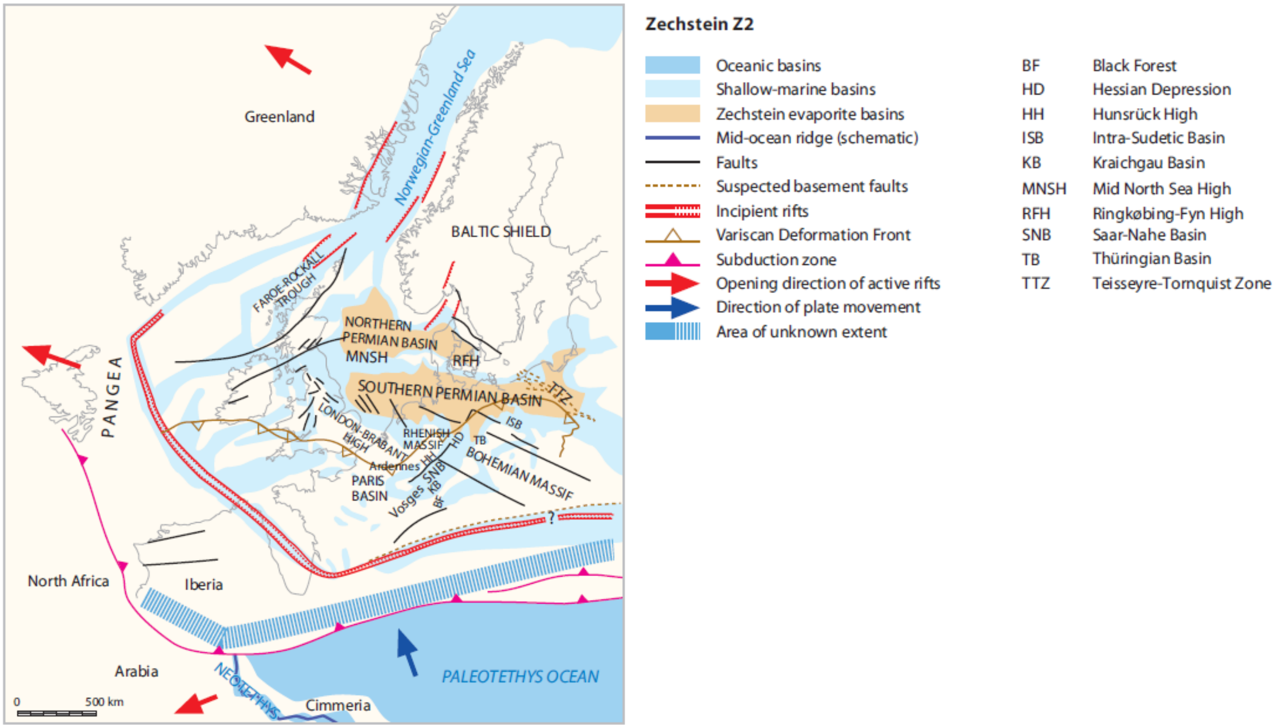

Figure 1.2. Location of the Southern Permian Basin during the deposition of the Zechstein 2 (Z2) cycle. Adjusted from Peryt et al., 2010.

1.2 Stratigraphy

The Zechstein consists of seven formations in total, of which five have been identified in the subsurface of the Netherlands. They are referred to as Z1-Z7, of which the Z1-Z5 consists of evaporite cycles in the basinal part. The presence of carbonates is limited to the lower three formation/cycles (Z1-Z3), which represents deposition in seawater of normal salinities and are not evaporitic. The evaporites that follow afterward reflect increasing salinities in the basin. The Z4 and Z5 are more playa-like deposits (Geluk, 2000) and the Z6 and Z7 are only present in Germany and Poland (Peryt et al., 2010).

The stratigraphy of the Zechstein deposits is illustrated in Figure 1.3. It can be seen here that the Zechstein cycles consist of a somewhat regular pattern of deposits: from base to top a claystone, followed by carbonates, anhydrites and halites (and ultimately magnesium-potassium salts). Variations in distribution and thickness between the different cycles can be observed. An example is the Z1 Halite, which is only present in a spatially limited belt running NW-SE through the southern onshore of the Netherlands and the lack of carbonates after the Z3, as mentioned earlier.

The names of the various formations differ a bit in each country. To simplify the work that has to be done, the division as encountered in the Netherlands will be used. This is also well top data available from the Netherlands in which this division is used. Figure 1.4 shows this simplified version of the stratigraphy.

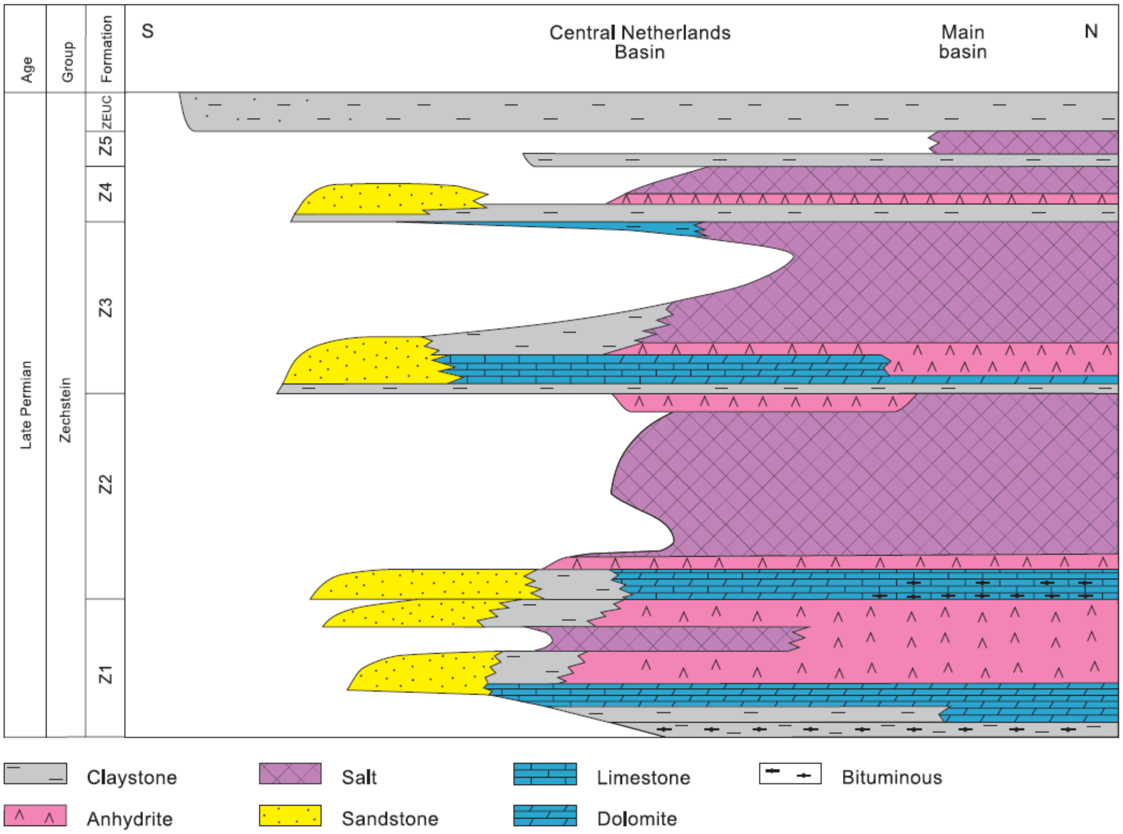

Figure 1.3. Stratigraphy of the Zechstein deposits in the Central Netherlands Basin, from De Jager et al. (2007).

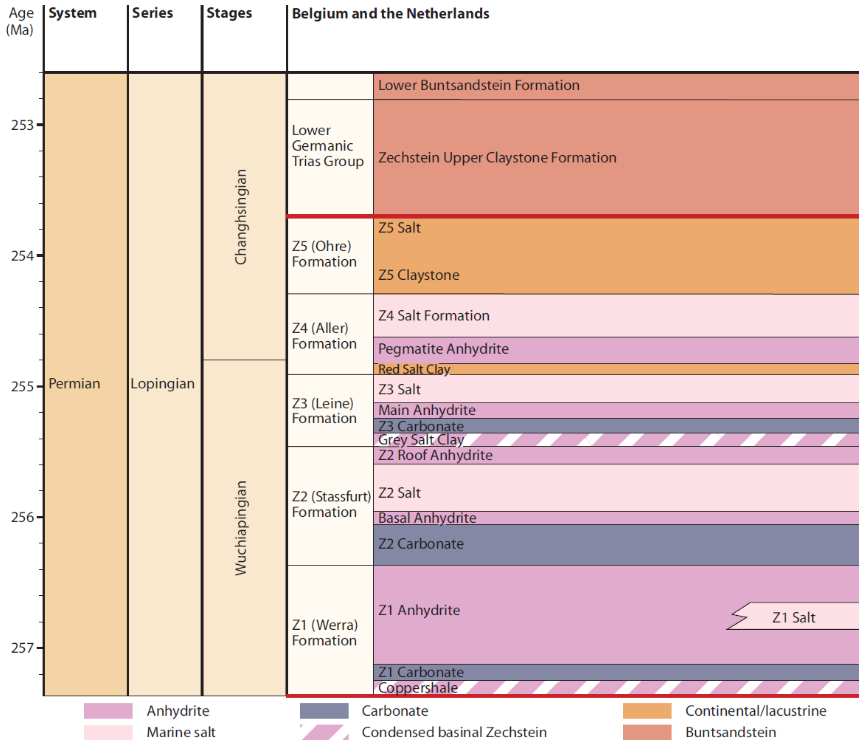

Figure 1.4. Simplified Zechstein stratigraphy based on the subsurface of the Netherlands. Modified after Peryt et al., 2010.

1.3 Salinity of the ocean

An important input into the model is the composition of Permian seawater during the deposition of the Zechstein. Present-day seawater has an average total salt concentration of 35.05 kg/m^3 (Leeder, 1999), but the total amount of major ions in seawater have changed throughout time (Warren, 2016; Hay et al., 2006).

The salinity of the ocean during the Phanerozoic has been reconstructed using the content of chlorine in the oceans over time, where the chloride ion is assumed to be the only ion that is restricted to the ocean. The salinity of the ocean is dependent on two variables, first of all the amount of water that is present in the oceans and secondly the amount of salt that is dissolved in the oceans. By determining the size of all salt deposits on Earth and the water volumes of the oceans over time, a reconstruction of the salinity of the ocean can be made. Two models are considered to construct the salinity through the Phanerozoic; model A assumes no loss of water through subduction and model B assumes a steady loss of water through subduction (but no loss of salts dissolved in the water). This gives average salinities of 43.78 ppt and 41.86 ppt for the Late Permian (model A and model B respectively; Hay et al., 2006). Figure 1.5 shows this change in salinity through time.

The concentrations of minerals dissolved in present-day seawater are given in Figure 1.6, which also shows the order in which the different minerals precipitate under conditions of progressing evaporation. The relative concentrations of the minerals dissolved in seawater were probably the same, as no indication to suggest otherwise is given. The concentrations were thus only higher.

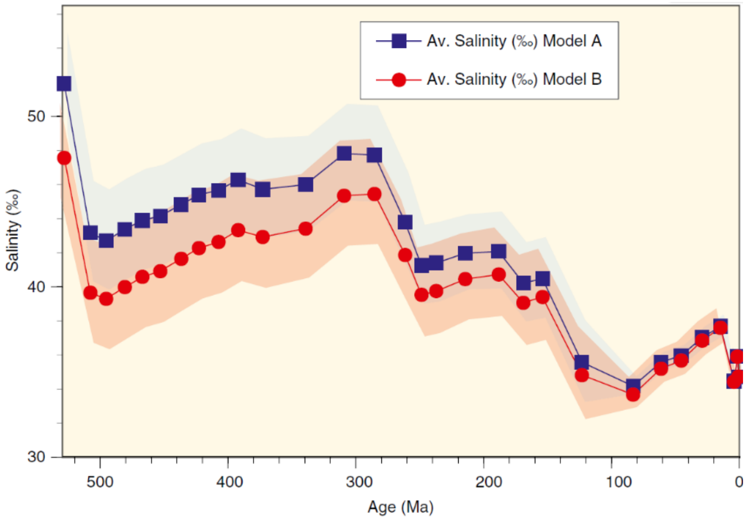

Figure 1.5. Average salinity of the oceans through time, from Warren (2016).

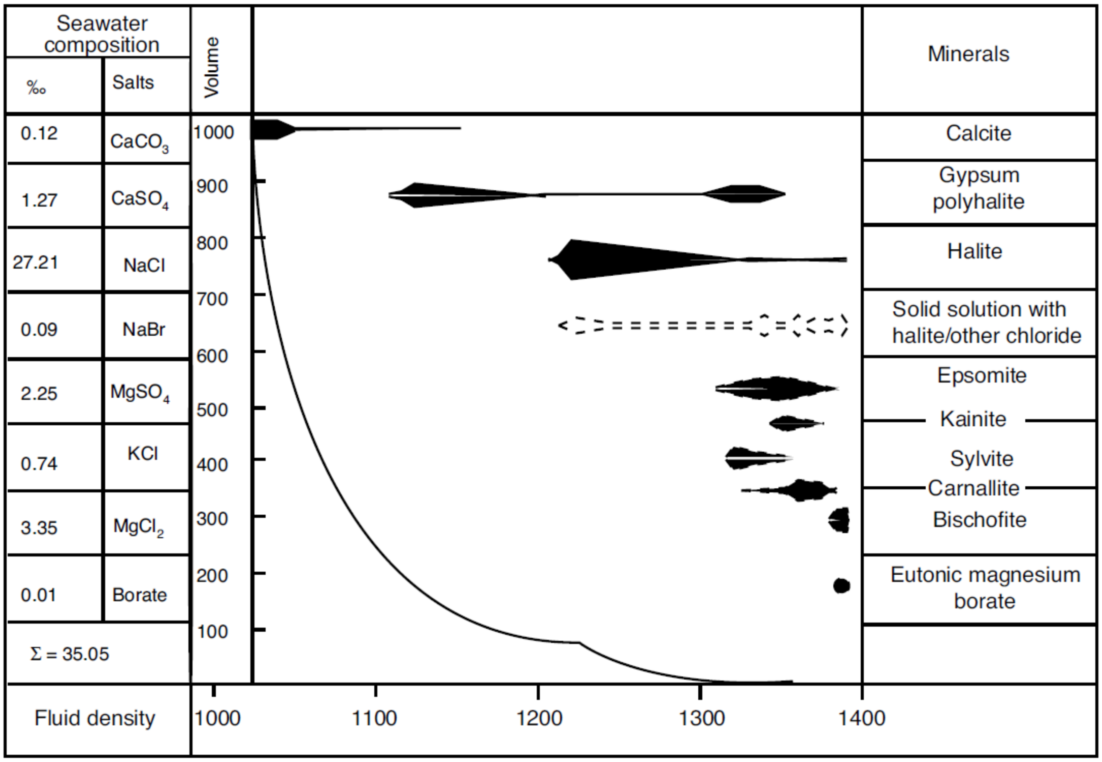

Figure 1.6. The concentrations of minerals dissolved in modern-day seawater is given on the left of the diagram and the order in which the different minerals are precipitated is given on the right of the diagram. From Leeder (1999).

1.4 Model set-up

To investigate the Zechstein basin architecture, a schematic model has been set up to explore the boundary conditions necessary to understand the basin and its dynamics. This model is illustrated in Figure 1.4. The SPB has a connection and a flux to the ocean, both the SPB and the ocean have a certain salinity. The water in the basin evaporates and minerals dissolved in the water precipitate and form certain volumes of sediment. The basin itself furthermore subsides whereby the assumption is made that the top of the sediment stays constant.

The input necessary to explore this model are thus the volumes of the deposits and their lithologies, the size of the basin, the salinities of the various water sources and the evaporation rate.

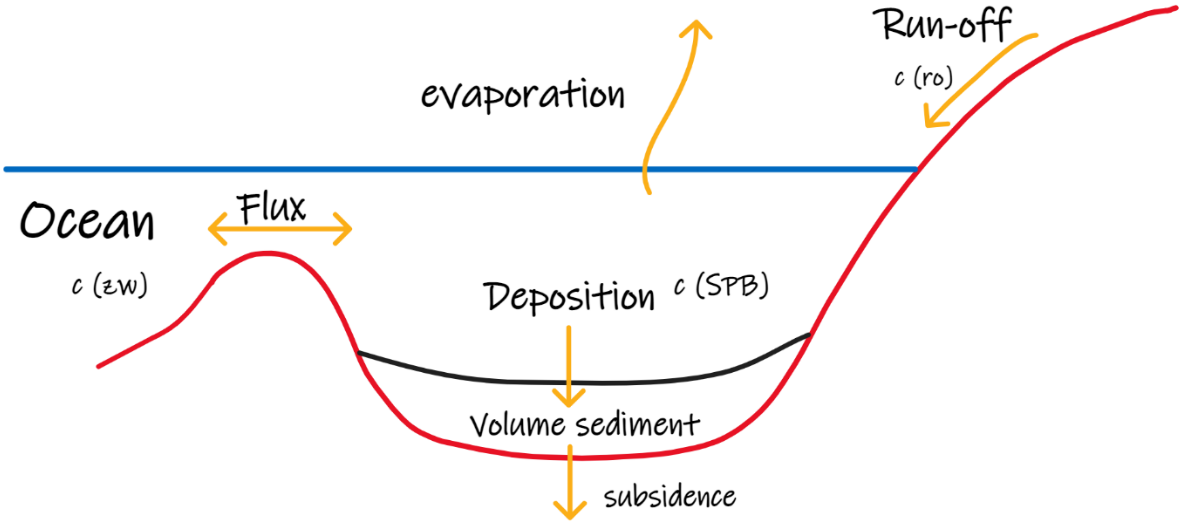

Figure 1.7. Model set-up. Blue line represents the water level in the basin and the ocean, the red line represents the boundaries of the basin, the black line represents the top of the sediment and the yellow arrows represent the fluxes in the basin. c (zw) = salinity of the sea water, c (SPB) = the salinity within the SPB and c (ro) = the salinity of the run-off water.

2 Method

In the following subsections the methods used for the quantitative analysis of the Zechstein basin are described in more detail. Determining and calculating the volumes of the different Zechstein sediments is described in the first step (Section 2.1). Using this information, the concentrations of the different element in Permian seawater and their saturation concentrations, the minimal water volumes necessary for deposition of these sediments (Section 2.2) and the minimal duration of deposition (Section 2.3) are calculated. All these calculations are the basis for the investigation of the basin dynamics during the deposition of the Zechstein, which is done by investigating the accommodation space in the basin. In order to do so, cross sections through the Zechstein in the subsurface of the Netherlands are made (Section 2.4) and adjusted for vertical response as predicted by the isostatic balance (Section2.4.1).

The values for all input parameters can be found in Table 2.3.

2.1 Volume calculations

In order to improve our understanding of the basin architecture and possibly dynamics during the deposition of the Zechstein, the volumes of the various units/members need to be calculated. There is a lot of uncertainty within these calculations, but the best effort is made to come to a decent estimation. One uncertainty that is not taken into account is the effect of erosion. As discussed in the introduction (see Section 1.2) the stratigraphy has been simplified.

Table 2.1. The data that is used for calculating/determining the surface area and volumes of the various Zechstein units. The figures under the heading "Surface area" are from the Southern Permian Basin Atlas (SPBA; Peryt et al., 2010) and can be found in the Appendices. The description and codes of the well top data can be found in Table 2.2.

		Surface area	Volume
Z1	Kupferschiefer	SPBA fig. 8.6	Well tops data from the Netherlands, ZEZ1K unit
	Carbonate/limestone	Figure 6.2	Figure 6.2
	Anhydrite	Figure 6.2	Well tops data from the Netherlands, ZEZ1A+ZEZ1W+ZEZ1T units
	Halite	Figure 6.2	Well tops data from the Netherlands, ZEZ1H unit
Z2	Carbonates and equivalents	Figure 6.3 and Figure 6.4	Figure 6.3 and Figure 6.4
	Lower anhydrite	Figure 6.3	Well tops data from the Netherlands, ZEZ2A unit
	Salt/halite	Figure 6.3	Well tops data from the Netherlands, ZEZ2H unit
	Roof anhydrite	Figure 6.3	Well tops data from the Netherlands, ZEZ2T unit
Z3	Grey salt clay	Figure 6.5	Well tops data from the Netherlands, ZEZ3G unit
	Carbonate	Figure 6.5	Figure 6.5
	Anhydrite	Figure 6.5	Well tops data from the Netherlands, ZEZ3A unit
	Salt/halite	Figure 6.5	Well tops data from the Netherlands, ZEZ3H unit
Z4	Red salt clay	Figure 6.6	Well tops data from the Netherlands, ZEZ4R unit
	(Pegmatite) anhydrite	Figure 6.6	Well tops data from the Netherlands, ZEZ4A unit
	Salt/halite	Figure 6.6	Well tops data from the Netherlands, ZEZ4H unit
Z5	Claystone	Figure 6.6	Well tops data from the Netherlands, ZEZ5H unit
	Halite	Figure 6.6	Well tops data from the Netherlands, ZEZ5R unit

The volumes of the different Zechstein units are not all calculated in the same manner, which will be described below in Sections 2.1.1 and 2.1.2. Which dataset is used for which formation is summarized in Table 2.1.

2.1.1 Volume calculations using thickness and distribution maps

For several units, maps with thickness estimation (or at least ranges of thicknesses) are present in the Southern Permian Basin Atlas (SPBA; Peryt et al., 2010). These maps are used to calculate the volume of these units.

Table 2.2. Well top data (from TNO-GDN, 2022)

Code	Name (English)	Name (Dutch)
ZEZ1K	Coppershale Member	Koperschalie Laagpakket
ZEZ1A	Z1 Lower Anhydrite Member	Z1 Onder-Anhydriet Laagpakket
ZEZ1W	Z1 Anhydrite Member	Z1 Anhydriet Laagpakket
ZEZ1T	Z1 Upper Anhydrite Member	Z1 Boven-Anhydriet Laagpakket
ZEZ1H	Z1 Salt Member	Z1 Zout Laagpakket
ZEZ2A	Z2 Basal Anhydrite Member	Z2 Basale Anhydriet Laagpakket
ZEZ2H	Z2 Salt Member	Z2 Zout Laagpakket
ZEZ2T	Z2 Roof Anhydrite Member	Z2 Dakanhydriet Laagpakket
ZEZ3G	Grey Salt Clay Member	Grijze Zoutklei Laagpakket
ZEZ3A	Z3 Main Anhydrite Member	Z3 Hoofdanhydriet Laagpakket
ZEZ3H	Z3 Salt Member	Z3 Zout Laagpakket
ZEZ4R	Red Salt Clay Member	Rode Zoutklei Laagpakket
ZEZ4A	Z4 Pegmatite Anhydrite Member	Z4 Pegmatiet-Anhydriet Laagpakket
ZEZ4H	Z4 Salt Member	Z4 Zout Laagpakket
ZEZ5R	Z5 Salt Clay Member	Z5 Zoutklei Laagpakket
ZEZ5H	Z5 Salt Member	Z5 Zout Laagpakket

The area size of the different polygons are calculated. Each of these polygons have a range of various thicknesses attributed to them, which are the minimum and maximum thickness in that specific polygon. Using this minima, maxima and averages gives the total minimum, maximum and average thickness of that formation/member. For example, a polygon with a surface area of 100 m^2 and a thickness range of 10-20 m (average is 15 m) will have a minimum volume of 1000 m^3, a maximum of 2000 m^3 and an average volume of 1500 m^3.

2.1.2 Use of well tops from the subsurface in the offshore Netherlands

To calculate the total volume of sediments in the Z1-Z5 formations, the size of the areas of the formations as described above are used. For the claystones and anhydrites it is assumed that they are distributed over the same area as the carbonates, while the distribution for the halites is more limited to the slope and the basin (in case of the Z1 Halite) or to the platform, slope and basin and not for the deposits lying more land inwards than the platform (in case for the Z2 and Z3 Halites). For the Z4 and Z5 Halites the same areas as used for the anhydrites are taken.

For these volume calculations the thicknesses of these units in the subsurface of the Netherlands are used, based on well tops data. The fringe formations are not used, and neither the formations that describe a unit in which a distinction between two different units cannot be made (e.g., the Z1 Anhydriet/Carbonaat laagpakket, in which it is not possible to distinguish between the Z1 Anhydrite and the Z1 Carbonate; TNO-GDN, 2022) This is all summarized in Table 2.2.

From the well top data the minimum, maximum and average thicknesses are calculated. When a formation is described using several units in the subsurface of the Netherlands, which is the case for the Z1 Anhydrite, the minima, maxima and averages of all those layers together are taken to get the final values.

To establish the volumes of these formations, the volumes in the offshore subsurface of the Netherlands of these formations are determined, which will then be extrapolated to the whole basin.

The following two steps are performed first:

1. The minimum, maximum and average thicknesses of each of the formations in each offshore block is determined using the Basis Registratie (Brh_Stratigrafie) database of EBN ($t_{formation\_block}$).
2. The area of each formation in each offshore block is determined by aggregating the offshore license blocks of the Netherlands and the surface areas of the formations from the SPBA in ArcGISPro ($A_{formation\_block}$).

The thickness and surface area of each formation in each offshore license block are multiplied to get the volume in each offshore block according to Equation 2.1:

$$[2.1]\ V_{formation\_block} = t_{formation\_block} \cdot A_{formation\_block}$$

$V_{formation\_block}$ = *the volume of each formation in each license block in the offshore Netherlands* (m^3)
$t_{formation\_block}$ = *the thickness of each formation in each license block in the offshore Netherlands* (m)
$A_{formation\_block}$ = *the surface area of each formation in each license block in the offshore Netherlands* (m^2)

For each formation the volumes in each block are summed to get the total volume of that formation in the Netherlands according to Equation 2.2:

$$[2.2]\ V_{formation\_NL} = \sum V_{formation\_block}$$

$V_{formation\_NL}$ = *the volume of each formation in the offshore Netherlands* (m^3)

The next step is to determine what fraction of each formation is present in the offshore Netherlands, in proportion relative to the whole SPB. Thus the area of that formation in the offshore Netherland is divided by the total area of the formation in the SPB to get the fraction according to Equation 2.3:

$$[2.3]\ f_{formation\_NL} = A_{formation\_NL}/A_{formation\_SPB}$$

$f_{formation\_NL}$ = *fraction of each formation in the Netherlands relative to the whole SPB*
$A_{formation\_NL}$ = *the surface area of each formation in the offshore Netherlands* (m^2)
$A_{formation\_SPB}$ = *the surface area of each formation in the SPB. See Table 2.1 for which data is used to compile these surface areas* (m^2)

For each formation, the volume of that formation in the offshore Netherlands is divided by this fraction to get the total volume in the SPB according to Equation 2.4:

$$[2.4]\ V_{formation\_SPB} = V_{formation\_NL} / f_{formation\_NL}$$

$$V_{formation\_SPB} = \text{the volume of each formation in the whole SPB } (m^3)$$

The volume of each formation in the SPB has been attributed a minimum, maximum and average value.

2.2 Water volume calculations

To be able to investigate the basin dimensions and dynamics, information regarding the amount of water necessary for deposition of the different lithologies are necessary. This can provide insights into the basin dynamics by comparing the volumes of water with the expected dimensions of the basin. To identify the minimum amount of water necessary for deposition of the different lithologies, the next parameters are required:

- Volumes of the different lithologies
- Densities of the lithologies
- Concentration at saturation of the different lithologies in Permian seawater

With this information, the amount of water that contains the necessary amount of elements for deposition of the carbonates, anhydrites and halites can be calculated. It is unfortunately not possible to calculate the amount of water necessary for deposition of the clays, as no known concentration of the elements necessary for deposition in water are known, and these deposits are most likely deposited by different processes. Furthermore, it is assumed that all elements are brought into the basin through the connection to a marine source.

All the values necessary for the calculations named below can be found in Table 2.3.

First, it will be assumed that all the anhydrite that is present now in the subsurface was actually deposited as gypsum, thus a volumetric correction must be performed. Gypsum dehydration to anhydrite causes a volume reduction of 39% (Azam, 2007), thus the volume of anhydrite must be multiplied with a factor of 1.39 to account for this dehydration. This is described by Equation 2.5:

$$[2.5]\ V_{gypsum} = V_{anhydrite} \cdot 1.39$$

$$V_{gypsum} = \text{the volume of gypsum} (m^3)$$
$$V_{anhydrite} = \text{the volume of anhydrite } (m^3)$$

Afterwards the mass of the evaporites can be calculated using Equation 2.6:

$$[2.6]\ m_{evaporite} = V_{evaporite} \cdot \rho$$

$$m_{evaporite} = \text{mass of the evaporite (kg)}$$
$$V_{evaporite} = \text{volume of the evaporite } (m^3)$$
$$\rho_{evaporite} = \text{the density of the evaporite } (kg/m^3)$$

When the total salt concentration in the basin reaches the saturation point of each type of evaporite, that type of evaporite will start to deposit. E.g., when the total salt concentration in the basin reaches 145 kg/m^3 gypsum will start to deposit instead of carbonate (see Table 2.3 for all saturation values). All the salt that enters the basin in excess of that saturation concentration is deposited (Topper & Meijer, 2013).

This is however not the case for the deposition of the carbonates, as the carbonates in the Zechstein are biogenic and are thus deposited by a different process. The accompanying equation used for calculating the amount of water necessary for the deposition of the carbonate is therefore slightly different from the equation used for the gypsum and halite. It must still be noted that this calculation is only valid if all elements for deposition of the carbonate are brought into the basin from a marine connection. This is also the case for the deposition of the gypsum and the halite, but more important to note for the carbonate.

In seawater of normal (or in this case, Permian) salinities, carbonate is deposited without the need for the water in the basin to reach saturation concentrations. Nevertheless, the amount of building blocks necessary for deposition can still be calculated, only the concentration of carbonate in Permian seawater is used instead of the concentration at saturation. This is described by Equation 2.7a:

$$[2.7a]\ V_{water\_carbonate} = m_{carbonate} / c_{cb\_Permian\_seawater}$$

$V_{water\_carbonate}$ = *the volume of water necessary for deposition of the carbonate* (m^3)
$c_{cb\_Permian\_seawater}$ = *the concentration of carbonate in Permian seawater* (kg/m^3)

The concentration at saturation for the deposition the gypsum and halite can be found in Table 2.3. These values are independent of the concentration of the seawater and were thus not different in the Late Permian compared to today.

Using the mass and the concentration of the evaporite in Permian seawater at the time of saturation, the amount of water necessary for deposition of the evaporite (gypsum or halite) can be calculated using Equation 2.7b:

$$[2.7b]\ V_{water\_evaporite} = m_{evaporite} / c_{saturation\_evaporite}$$

$V_{water\_evaporite}$ = *the volume of water necessary for deposition of the evaporite* (m^3)
$c_{saturation\_evaporite}$ = *the concentration at saturation for deposition of the evaporite* (kg/m^3)

2.3 Duration of deposition

The basin model that is used is sketched in Figure 2.1. The values for the fluxes are amended for each of the three different evaporites: the carbonates, gypsums and halites. This model is most likely only representative for the deposition of the halites, as the salinity in the basin for the deposition of the carbonates and gypsums will at some point switch to the deposition of the next evaporite. This is not taken into account by this model, but it still allows for quick calculations and rudimentary interpretations of the fluxes, duration of deposition and dimension of the Zechstein basin. The calculations for the carbonates are moreover not representative, as these deposits are biogenic and not evaporitic. It is not certain by what process the carbonates are precipitated and the model used in these calculations might thus not be correct.

For these calculations the assumption is made that the surface area of the basin is equal to the surface area of the deposits, that all building blocks for deposition of the carbonate, gypsum and halite are brought into the basin from a marine source (thus not through run-off) and that there is only an influx and no outflux present.

The influx from an oceanic realm is represented by Q_0 and the evaporation flux is represented by Q_e, which can be calculated by multiplying the rate of net evaporation by the surface area of the basin. The latter is assumed to be the same area as the surface area of the deposit. This was most likely not the case, but no other information on the surface area of the Southern Permian Sea is known and thus this is considered the best approach for now.

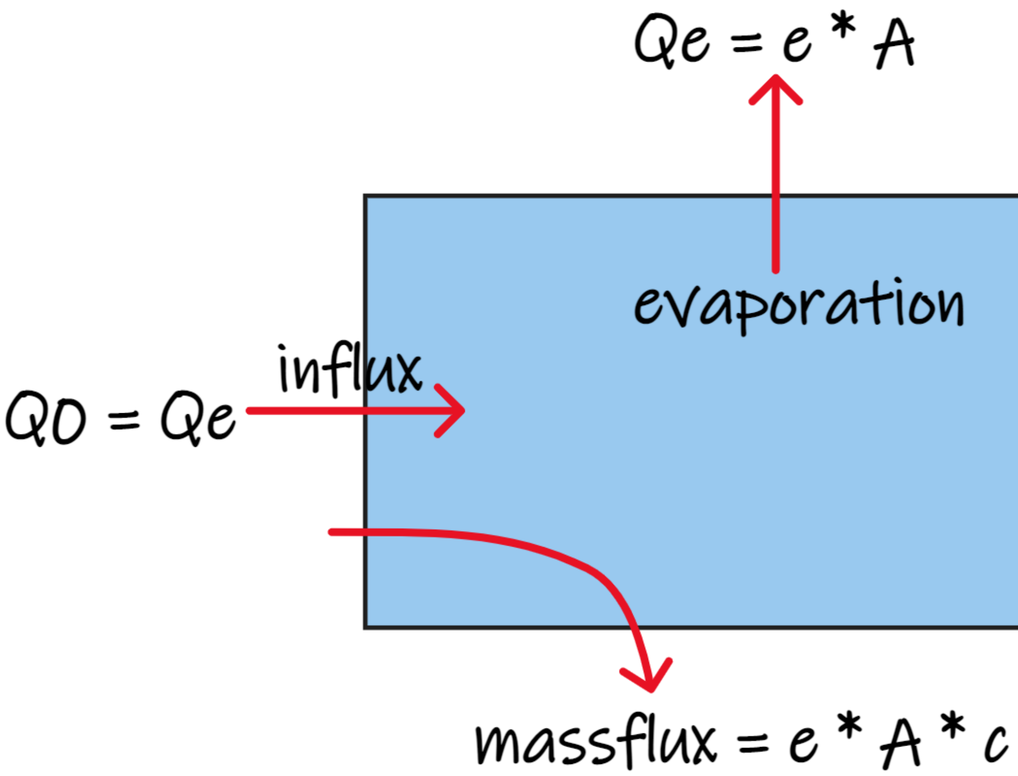

Figure 2.1. Simple model for calculations regarding the duration of deposition of the different evaporites. All equations and parameters are described in Equation 2.8, 2.9 and 2.10.

Assuming basin water volume is constant (and there is no effect of deposition or isostasy), it follows that the flux of incoming water is equal to the flux of evaporation, as described by Equation 2.8:

$$[2.8] \quad Q_0 = Q_e = e \cdot A$$

Q_0 = volume (in)flux of ocean water (m^3/yr)
e = rate of net evaporation (m/yr)
A = surface area of the basin (m^2)

Under the assumption that the basin is saturated for the evaporite, it follows that all the incoming salt will be subject to deposition. At any moment in time the mass flux of incoming salt is equal to the mass flux to the deposit, described by Equation 2.9:

$$[2.9] \text{ mass flux to deposit} = Q_0 \cdot S_{0\text{-}hal} = e \cdot A \cdot c_{evaporite\_Permian\_seawater} \, (kg/yr)$$

$c_{evaporite\_Permian\_seawater}$ = concentration of the evaporite in the incoming water (kg/m^3)

And with time the length of time needed to form the observed salt mass is described by Equation 2.10a:

$$[2.10a] \; m_{evaporite} = e \cdot A \cdot c_{evaporite\_Permian\_seawater} \cdot time$$

Time = duration of influx/deposition/evaporation (yr)
$m_{evaporite}$ = mass of the evaporite in the Zechstein basin (kg)

This can be rewritten into Equation 2.10b to be able to calculate the (minimum) duration of deposition for the observed mass of the evaporite. This is a minimum as this is the least amount of time necessary to deliver all the building blocks necessary for deposition and thus involves the assumption that the influx of water and the deposition of the evaporite is a simultaneous and continuous process. This equation involves an assumption for the net evaporation rate.

$$[2.10b]\ time = m_{evaporite}/(e \cdot A \cdot c_{evaporite\_Permian\_seawater})$$

In order to check whether the evaporation rate that is used is somewhat realistic, Equation 2.10a can be rewritten into Equation 2.10c. In this case an assumption must be made regarding the *time*.

$$[2.10c]\ e = m_{evaporite}/(A \cdot c_{evaporite\_Permian\_seawater} \cdot time)$$

The duration of the periods in which the various salts deposited is yet unknown and can be estimated crudely only. Alternatively, *the duration* can be calculated using assumed rates of deposition. The assumption in calculating the net evaporation rate (Equation 2.10c) is thus not *time*, but the deposition rate. As the Zechstein carbonates are biogenic and is thus most likely deposited by a different process than the gypsums and halite, there is no known deposition rate and the evaporation rate can thus not be checked for the carbonates.

In this case a new flux is introduced, which is the flux of deposition and can be calculated by multiplying the surface area of the evaporite and the deposition rate, as describe by Equation 2.11:

$$[2.11]\ Q_d = d \cdot A$$

Q_d = volume (in)flux of salt to the deposit (m^3/yr)
d = rate of deposition (m/yr)
A = surface area of the deposit (m^2)

Time can afterwards be calculated by using Equation 2.12:

$$[2.12]\ time = V_{evaporite}/Q_d = V_{evaporite}/(d \cdot A)$$

$V_{evaporite}$ = volume of the evaporite (m^3)

Combining Equation 2.10c and 2.12 allows for the evaporation rate to be directly related to the rate of deposition. This gives a new Equation 2.13:

$$[2.13]\ e = m_{evaporite} \cdot d \cdot A /(A \cdot c_{evaporite\_Permian\_seawater} \cdot V_{evaporite}) = (\rho_{evaporite} \cdot d)/c_{evaporite\_Permian\_seawater}$$

$\rho_{evaporite}$ = the density of the evaporite (kg/m^3)

This equation shows that the net evaporation rate is only dependent on the deposition rate, the concentration of the evaporite in the incoming water and the density of the evaporite. This leads to a constant evaporation rate for each of the Zechstein evaporite deposits (the gypsum and halite).

The deposition rate can also be calculated and compared to known deposition rates. Equation 2.13 can be rewritten to calculate the deposition rate, where the net evaporation rate is assumed. This is described by Equation 2.14:

$$[2.14]\ d = (e \cdot c_{evaporite\_Permian\_seawater})/\rho_{evaporite}$$

The values for the input parameters for all the equations mentioned above can be found in Table 2.3.

In both approaches $e \cdot A = Q_0$ can be calculated and can be compared to other straits, such as the strait of Gibraltar of the Bosphorus, to get an idea of the size of the connection between the Southern Permian Basin and the sea. For this the fluxes are recalculated in Sv, where 1 Sv is equal to 10^6 m^3/s (Meijer, 2006).

2.3.1 Duration until saturation is reached

To investigate whether there was only an influx of water into the basin or also an outflux present, it can be calculated how long it takes for the basin to reach salinity at the saturation point if only an influx is present. If this duration is significantly shorter, it can be concluded that an outflux is necessary for the basin to stay within the right salinity range for the deposition of the said evaporite.

For this the influx of water into the basin is needed, which is given by Equation 2.8. The dimensions of the basin are also necessary, but for this an assumption regarding average water depth in the basin is necessary. The dimensions of the basin can be calculated using Equation 2.15:

$$[2.15]\ V_{SPB} = D \cdot A$$

V_{SPB} = *the volume of the SPB* (m^3)
D = *the average water depth in the basin (m)*

If the total salinity in the basin reaches the saturation of gypsum, gypsum will start to precipitate instead of carbonate. If the total salinity in the basin reaches the saturation of halite, halite will start to precipitate instead of gypsum. The increase in total salinity per year is thus necessary to determine how long it will take to reach this saturation value. This is given by Equation 2.16:

$$[2.16]\ \Delta S_{SPB} = Q_0 \cdot S/V_{SPB} = e \cdot A \cdot S/(D \cdot A) = e \cdot S/D$$

ΔS_{SPB} = *the increase in total salinity of the SPB per year* ($kg/(m^3 \cdot yr)$)
S = *Total salt concentration of Permian seawater* (kg/m^3)

If carbonate is deposited, all excess carbonate goes to the deposit and thus there is no increase in carbonate in the SPB. Formula 17 thus needs to be adjusted for this, which is described by Equation 2.17:

$$[2.17]\ \Delta S_{SPB\_cb} = e \cdot S/D - e \cdot c_{cb\_Permian\_seawater}/D$$

ΔS_{SPB_cb} = *the increase in total salinity of the SPB per year if carbonate is the mineral that precipitates* ($kg/(m^3 \cdot yr)$

In this case the total salinity in the basin at the beginning of the precipitation of carbonate is equal to the concentration of Permian seawater (S), as the Zechstein carbonate is not evaporitic. The precipitation of carbonate stops if the total salinity in the basin is equal to the concentration at saturation of gypsum ($S_{SPB} = S_{gy}$), which is not necessarily the case for the deposition of gypsum and halite (see Figure 1.7). This increase in salinity over the time can be described by Equation 2.18:

$$[2.18]\ S_{SPB} = S + \Delta S_{SPB\_cb} \cdot t$$

S_{SPB} = *the total salinity in the SPB* (kg/m^3)
t = *time (yr)*

This can be rewritten to get the amount of time it takes for the total salt concentration in the basin to reach the saturation of gypsum by Equation 2.19:

$$[2.19]\ t = (S_{SPB} - S_{cb})/\Delta S_{SPB\_cb}$$

It must be noted that the outcome of this calculation is most likely not that reliable, as the carbonate is not evaporitic and is thus deposited by a different process than the evaporites. However, it still gives some indication to the salinity in the basin during the deposition of the carbonate

A similar calculation can be made if the gypsum is the mineral to precipitate, only now considering that the gypsum is an evaporite. The increase in salinity per year is given by Equation 2.20:

$$[2.20]\ \Delta S_{SPB\_gy} = e \cdot S/D - e \cdot c_{gy\_Permian\_seawater}/D$$

ΔS_{SPB_gy} = *the increase in total salinity of the SPB per year if gypsum is the mineral that precipitates (kg/(m^3·yr)*

In this case the total salinity in the basin at the beginning of the precipitation of gypsum is equal to the concentration at saturation of gypsum (S_{gy}). The precipitation of gypsum stops if the total salinity in the basin is equal to the concentration at saturation of halite ($S_{SPB} = S_{hal}$). This increase in salinity over the time can be described by Equation 2.21 and can be rewritten into the amount of time it takes for the salinity in the basin to reach the saturation of halite by Equation 2.22, where:

$$[2.21]\ S_{SPB} = S_{gy} + \Delta S_{SPB\_gy} \cdot t$$

$$[2.22]\ t = (S_{SPB} - S_{gy})/\Delta S_{SPB\_gy}$$

2.4 Accommodation space in the basin

To better understand how and in what kind of basin the Zechstein sediments were deposited, it requires to understand the variations in amount of accommodation space in the basin. This is both to apprehend the dimensions of the basin (and thus the type of basin) and why there is cyclicity in the Zechstein deposits.

The accommodation space in the basin is influenced by eustatic sea-level changes, variations in sedimentation rate and subsidence. Subsidence can be divided into two elements here: the tectonic and the isostatic subsidence. The tectonic subsidence in the case of the Zechstein is mostly due to thermal relaxation of the crust (Van Wees et al 2000, Peryt et al., 2010) and the isostatic subsidence is the subsidence due to loading of the crust by the overlying sediments and evaporites (Van den Belt & de Boer, 2007). Isostatic subsidence responds to load (the overlying weight of the sediments and evaporites) and is thus dependent on the rate in which this load applied. The rate of isostatic subsidence can thus vary in different locations, as the sedimentation rate can vary in different locations. This does not take the isostatic subsidence response time into account.

To be able to investigate the accommodation space in the basin, the focus is put on the Z1 cycle. A cross section through the Dutch offshore is constructed (for details on the construction of this cross section, see Section 2.4.1), from which a cross section through the Z1 cycle can be generated. Three pseudo-wells are established in this cross section, from which a plot can be constructed that shows the total thickness of the Z1 deposits in each well over time (the time aspect is the calculated duration of deposition as described in Section 2.3). The Kupferschiefer has been estimated to have been deposited in 17 kyr (Hirst and Dunham, 1963). The slope of the lines in this plot represents the sedimentation rate in that pseudo-well over time. This curve essentially represents how fast the accommodation space is filled and thus provides information on the amount of accommodation space present in the basin during the deposition of the Z1 cycle over time. Changes in the slope of this curve either indicate eustatic sea-level changes, isostatic or tectonic subsidence or could suggest that the basin (partly) filled up and there is thus no more accommodation space left. Eustatic sea-level changes are ignored, as this requires an amount of detail that unfortunately does not fit within the scope of this project. The vertical response of the basin as predicted by the isostatic balance can be adjusted for using the Airy isostasy model as described by Van den Belt & de Boer (2007). This is described in more detail in Section 2.4.1.

If the remainder of the curve still shows a slope and/or a change in slope, this could either indicate that the basin is (partly) filled up, that a tectonic subsidence competent is present or that the effect of eustatic sea-level changes is too significant to be ignored.

2.4.1 Construction of the cross section

A cross section through the Dutch offshore has been constructed to investigate basin architecture during the deposition of the Zechstein. Using the Basis Registratie (Brh_Stratigrafie) database of EBN the thickness of each Zechstein deposit in the subsurface can be determined in each license block. An imaginary line is drawn through the following license blocks, representing the cross-section, from north to south:

A12 - A15 - A18 E03 - E06 - E09 - E12 - E15 - E18 - K03 - K06 - K09 - K12 - K15 - K18 - P03 - P06 - P09 - P12 - P15

Attributing a thickness to each of the Zechstein deposits in these blocks gives a rudimentary cross section through the Zechstein. The cross section is cleaned up a bit, as in some blocks either no data is present and/or part of the sediments might have eroded away or are distributed differently (can be the case for the halite, due to salt tectonic).

The vertical response of the Z1 Carbonate, Anhydrite and Halite deposits as predicted by the isostatic balance can thus be adjusted for using the model as described by Van den Belt & de Boer (2007). Sedimentation and isostatic compensation are considered to be syn-depositional processes, although the isostatic response time is around 10 kyr (Watts, 2001, as cited in Van den Belt & de Boer, 2007). The isostatic subsidence due to halite precipitation will be discussed first, followed by the subsidence due to anhydrite and carbonate.

2.4.1.1 Isostatic subsidence due to halite precipitation

Halite precipitation is very fast and thus may fill a basin quickly, leading to a subsidence response, creating more accommodation space, etc. This process is continued until either no more water is supplied or the sedimentation rate is faster than the subsidence, and thus no accommodation space is present to deposit the halite (Van den Belt & de Boer, 2007). This process is described by Figure 2.2. A schematic drawing of the isostatic balance before and after the deposition of the halite is given in Figure 2.3, from which an equation can be derived in which the original basin depth that is necessary for a certain amount of halite deposits can be calculated, as described by Equation 2.23:

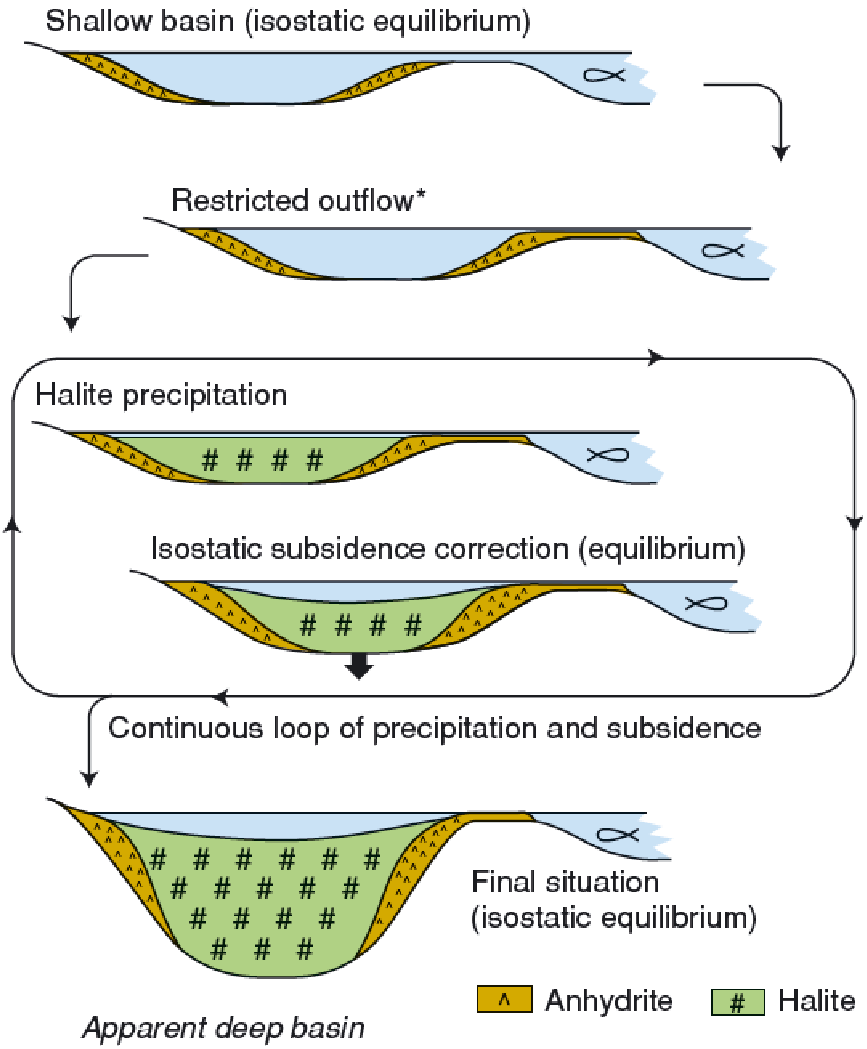

Figure 2.2. Halite precipitation and its effect on the isostatic balance. From Van den Belt & de Boer (2007).

$$[2.23]\ D_{basin} \cdot \rho_{water} + H_{asthenosphere} \cdot \rho_{asthenosphere} = Th_{halite} \cdot \rho_{halite}$$

$$D_{basin} \cdot \rho_{water} + (Th_{halite} - D_{basin}) \cdot \rho_{asthenosphere} = Th_{halite} \cdot \rho_{halite}$$

$$D_{basin} \cdot \rho_{water} + Th_{halite} \cdot \rho_{asthenosphere} - D_{basin} \cdot \rho_{asthenosphere} = Th_{halite} \cdot \rho_{halite}$$

$$Th_{halite}\,(\rho_{asthenosphere} - \rho_{halite}) = D_{basin} \cdot \rho_{asthenosphere} - D_{basin} \cdot \rho_{water}$$

$$Th_{halite}\,(\rho_{asthenosphere} - \rho_{halite}) = D_{basin} \cdot (\rho_{asthenosphere} - \rho_{water})$$

$$Th_{halite} = D_{basin} \cdot ((\rho_{asthenosphere} - \rho_{water})/(\rho_{asthenosphere} - \rho_{halite}) = 2.1 \cdot D_{basin}$$

Th_{halite} = the thickness of halite (m)
D_{basin} = the original water depth of the basin (m)
ρ_{water} = the density of seawater (kg/m^3)
ρ_{halite} = the density of halite (kg/m^3)

2.4.1.2 Isostatic subsidence due to anhydrite precipitation

The isostatic compensation for anhydrite is described by Figure 2.4, where a situation is sketched in which there is a balance between subsidence and sedimentation in an aggradational-platform. If the salinity of the basin reaches the saturation for anhydrite/gypsum, this balance will be distorted. Gypsum mainly precipitates on the slope of the underlying sediments and anhydrite mainly on the platform, due to certain chemical conditions. The density of anhydrite is significantly larger to that of average sediment (2.9 versus ~2.2 kg/m^3) and thus when anhydrite starts to precipitate, it exerts an accelerated load on the lithosphere (Van den Belt & de Boer, 2007). A schematic drawing of the isostatic balance before and after the deposition of the anhydrite is given in Figure 2.5and the equation that describes this disturbance of the isostatic balance and the increased thickness of the anhydrite is described by Equation 2.24:

$$[2.24]\ Th_{sediment} \cdot \rho_{sediment} + H_{asthenosphere} \cdot \rho_{asthenosphere} = Th_{anhydrite} \cdot \rho_{anhydrite}$$

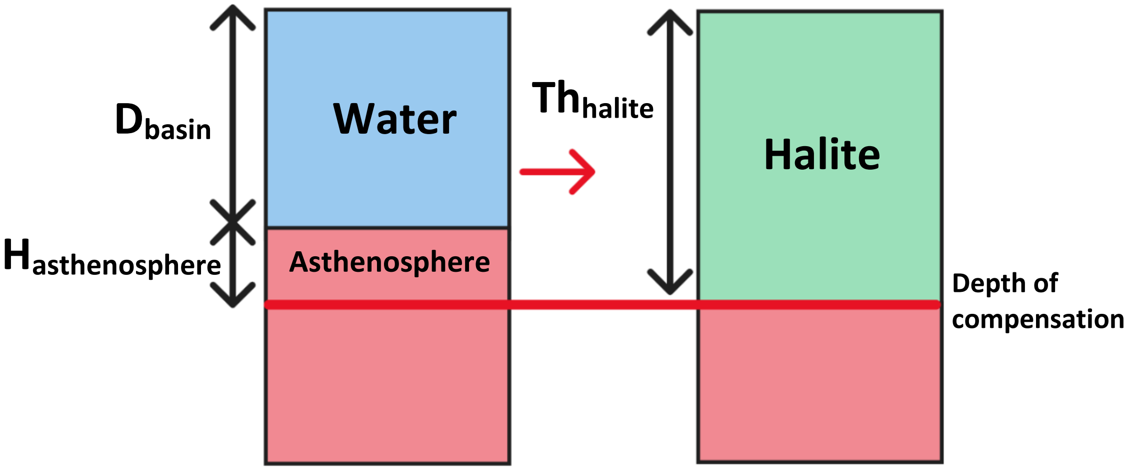

Figure 2.3. Schematic drawing of the Airy isostasy model for the Zechstein halite, as described by Van den Belt & de Boer (2007). Each of the different components (the water, halite and asthenosphere) have a certain density. The equation that describes this situation is Equation 2.23. Note: the drawing is not to scale.

Th_{halite} = the thickness of the halite deposit, D_{basin} = the original water depth of the basin, $H_{asthenosphere}$ = the distance from the bottom of the basin to the depth of compensation.

$$Th_{sediment} \cdot \rho_{sediment} + (Th_{anhydrite} - Th_{sediment}) \cdot \rho_{asthenosphere} = Th_{anhydrite} \cdot \rho_{anhydrite}$$

$$Th_{sediment} \cdot \rho_{sediment} + Th_{anhydrite} \cdot \rho_{asthenosphere} - Th_{sediment} \cdot \rho_{asthenosphere} = Th_{anhydrite} \cdot \rho_{anhydrite}$$

$$Th_{anhydrite} (\rho_{asthenosphere} - \rho_{anhydrite}) = Th_{sediment} \cdot \rho_{asthenosphere} - Th_{sediment} \cdot \rho_{sediment}$$

$$Th_{anhydrite} (\rho_{asthenosphere} - \rho_{anhydrite}) = Th_{sediment} \cdot (\rho_{asthenosphere} - \rho_{sediment})$$

$$Th_{anhydrite} = Th_{sediment} \cdot ((\rho_{asthenosphere} - \rho_{sediment})/(\rho_{asthenosphere} - \rho_{anhydrite}) = 3.1 \cdot Th_{sediment}$$

$Th_{anhydrite}$ = *the thickness of anhydrite (m)*
$Th_{sediment}$ = *the thickness of sediment (m)*
$\rho_{asthenosphere}$ = *the density of the asthenosphere* (kg/m^3)
$\rho_{sediment}$ = *the density of sediment* (kg/m^3)
$\rho_{anhydrite}$ = *the density of anhydrite* (kg/m^3)

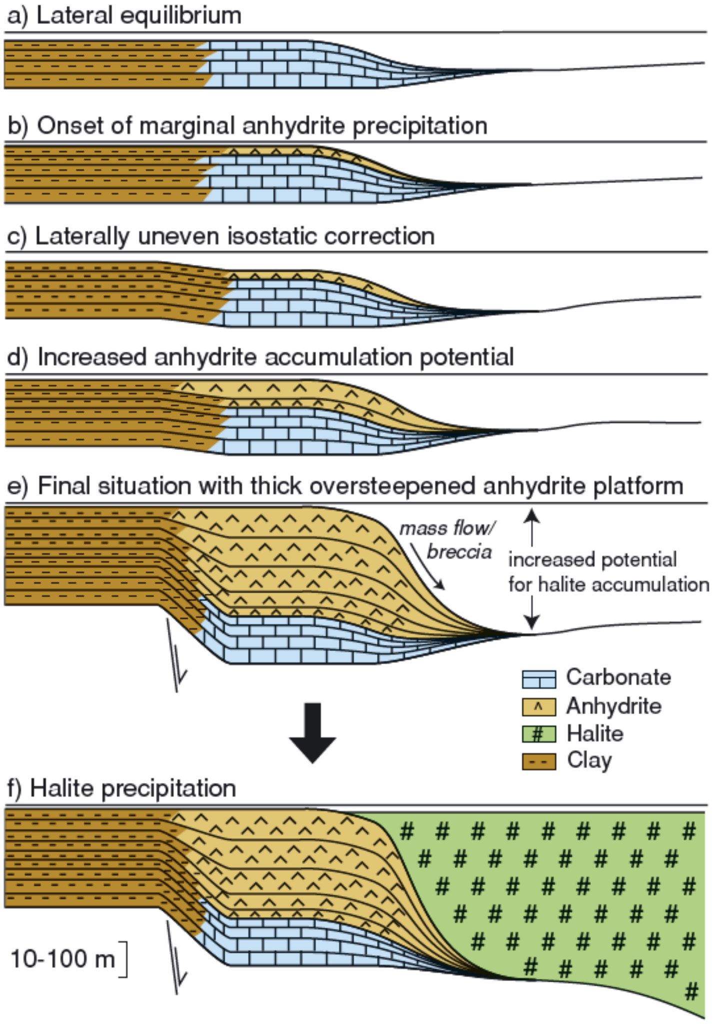

Figure 2.4. The precipitation of anhydrite and its effect on the isostatic balance. From Van den Belt & de Boer (2007).

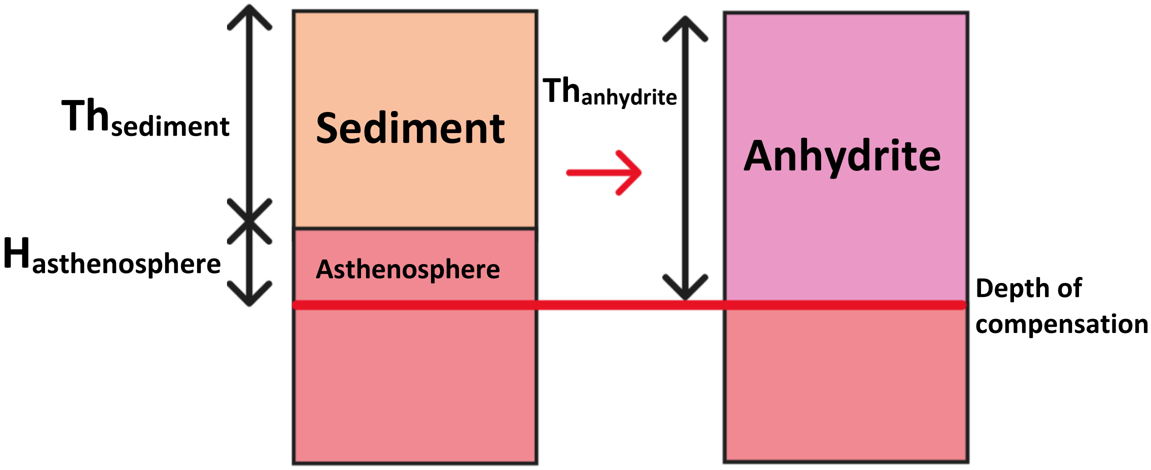

Figure 2.5. Schematic drawing of the Airy isostasy model for the Zechstein anhydrite, as described by Van den Belt & de Boer (2007). Each of the different components (the sediment, anhydrite and asthenosphere) have a certain density. The equation that describes this situation is Equation 2.24. Note: the drawing is not to scale.

$Th_{anhydrite}$ = the thickness of the anhydrite deposit, $Th_{sediment}$ = the thickness of the sediment, $H_{asthenosphere}$ = the distance from the bottom of the basin to the depth of compensation.

2.4.1.3 Isostatic subsidence due to carbonate deposition

The isostatic subsidence and associated isostatic balance are not described by Van den Belt & de Boer (2007), but can derived from the same equations as for the isostatic subsidence for the halite and anhydrite. A schematic drawing of the isostatic balance before and after the deposition of the carbonate is given in Figure 2.6 and the equation that describes this disturbance of the isostatic balance and the increased thickness of the carbonate is described by Equation 2.25:

$$[2.25]\ H_{water} \cdot \rho_{water} + H_{asthenosphere} \cdot \rho_{asthenosphere} = Th_{carbonate} \cdot \rho_{carbonate}$$

$$H_{water} \cdot \rho_{water} + (Th_{halite} - D_{basin}) \cdot \rho_{asthenosphere} = Th_{carbonate} \cdot \rho_{carbonate}$$

$$H_{water} \cdot \rho_{water} + Th_{halite} \cdot \rho_{asthenosphere} - H_{water} \cdot \rho_{asthenosphere} = Th_{carbonate} \cdot \rho_{carbonate}$$

$$Th_{carbonate}\,(\rho_{asthenosphere} - \rho_{carbonate}) = H_{water} \cdot \rho_{asthenosphere} - D_{basin} \cdot \rho_{water}$$

$$Th_{carbonate}\,(\rho_{asthenosphere} - \rho_{carbonate}) = H_{water} \cdot (\rho_{asthenosphere} - \rho_{water})$$

$$Th_{carbonate} = H_{water} \cdot ((\rho_{asthenosphere} - \rho_{water})/(\rho_{asthenosphere} - \rho_{carbonate}) = 5.1 \cdot D_{basin}$$

$Th_{carbonate}$ = the thickness of carbonate (m)
H_{water} = the depth of the water from the top of the carbonate to the bottom of the basin (m)
ρ_{water} = the density of seawater (kg/m^3)
$\rho_{carbonate}$ = the density of carbonate (kg/m^3)

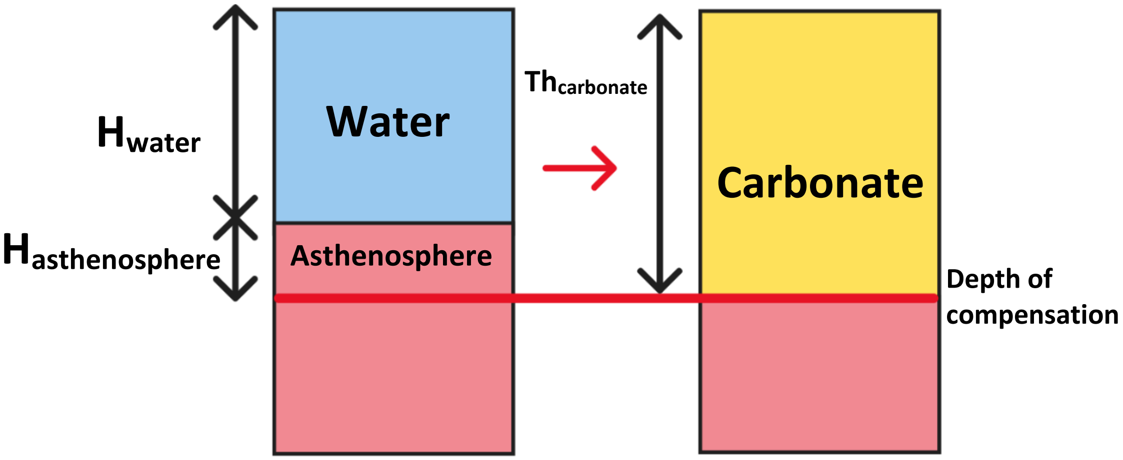

Figure 2.6. Schematic drawing of the Airy isostasy model for the Zechstein carbonate, as described by Van den Belt & de Boer (2007). Each of the different components (the water, carbonate and asthenosphere) have a certain density. The equation that describes this situation is Equation 2.25. Note: the drawing is not to scale.

$Th_{carbonate}$ = the thickness of the carbonate deposit, H_{water} = the depth of the water from the top of the carbonate to the bottom of the basin, $H_{asthenosphere}$ = the distance from the bottom of the basin to the depth of compensation.

Table 2.3. All input parameters

Parameter	Description	Value		Reference
S	Total salt concentration of Permian seawater (model B)	41.86	kg/m^3	Hay et al. (2006)
$A_{Z1\text{-}Z5}$	Surface area for each cycle	See Table 6.1		
e	Evaporation rate	2	m/yr	Babkin (2009)
$\rho_{asthenosphere}$	Density of the asthenosphere	3300	kg/m^3	
$\rho_{anhydrite}$	Density of anhydrite	2900	kg/m^3	Van den Belt & de Boer
ρ_{water}	Density of seawater	1030	kg/m^3	(2007
Carbonate ($CaCO_3$)				
ρ_{cb}	Density	2850	kg/m^3	Van den Belt & de Boer (2007)
$c_{cb\_Permian\_seawater}$	Concentration of carbonate in Permian seawater	0.14	kg/m^3	Leeder (1999); Hay et al. (2006)
$c_{saturation\_cb}$	Concentration of evaporitic carbonate at saturation	0.171	kg/m^3	Topper & Meijer (2013)
S_{cb}	Total salt concentration at saturation of evaporitic carbonate	50	kg/m^3	Warren (2016)
$d_{depo\_min\_cb}$	Slowest deposition rate (evaporitic carbonate)	0.5	mm/yr	Warren (2016)
$d_{depo\_max\_cb}$	Fastest deposition rate (evaporitic carbonate)	1	mm/yr	Warren (2016
Gypsum ($CaSO_4$)				
ρ_{gy}	Density	2300	kg/m^3	Topper & Meijer (2013)
$c_{gy\_Permian\_seawater}$	Concentration of gypsum in Permian seawater	1.52	kg/m^3	Leeder (1999); Hay et al. (2006)
$c_{saturation\_gy}$	Concentration of gypsum at saturation	5.25	kg/m^3	Topper & Meijer (2013)
S_{gy}	Total salt concentration at saturation of gypsum	145	kg/m^3	Topper & Meijer (2013)
$d_{depo\_min\_gy}$	Slowest deposition rate	1	mm/yr	Van den Belt & de Boer (2007)
$d_{depo\_max\_gy}$	Fastest deposition rate	10	mm/yr	Van den Belt & de Boer (2007); Warren (2016)
Halite ($NaCl$)				
ρ_{hal}	Density	2200	kg/m^3	Topper & Meijer (2013)
$c_{hal\_Permian\_seawater}$	Concentration of halite in Permian seawater	32.50	kg/m^3	Leeder (1999); Hay et al. (2006)
$c_{saturation\_hal}$	Concentration at saturation of halite	271.71	kg/m^3	Topper & Meijer (2013)
S_{hal}	Total salt concentration at saturation of halite	350	kg/m^3	Topper & Meijer (2013)
$d_{depo\_min\_hal}$	Slowest deposition rate	50	mm/yr	Warren (2016)
$d_{depo\_max\_hal}$	Fastest deposition rate	150	mm/yr	Manzi et al. (2012)

3 Results

3.1 Volumes of the Zechstein deposits

The average volumes of the most important deposits of the Zechstein are plotted per Zechstein cycle in Figure 3.1 and per type of deposit in Figure 3.2. All the data is summarized in Table 6.1 in the Appendices. A trend in the volumes of the Zechstein cycles can be identified in Figure 3.1, where the Z2 cycle is the volumetrically largest, the Z3 cycle is volumetrically smaller than the Z2 cycle, the Z4 cycle is again smaller than the Z3 cycle and the Z5 cycle is once again smaller than the Z4 cycle. Thus, from the Z2 onwards each cycle becomes volumetrically increasingly smaller. The Z1 cycle is the exception to this.

Zooming into the division of volumes within the cycles (see Figure 3.2), the trend that is described above is exactly present in the halites volumes. These deposits are also significantly larger than the other types of deposits and no such trend can be found in these other types of deposits. The trend that can be found in Figure 3.1 is thus controlled by the halite volumes as depicted in Figure 3.2.

3.2 Water volumes

Figure 3.3 shows the minimum amount of water necessary for deposition of all the Zechstein sediments (under the condition that all building blocks necessary for the deposition are coming from a marine source and that no other source is present). The results are plotted as the average water column necessary for deposition of the average volume of deposits, as this will give the best idea of the possible basin dimensions. All the data is summarized in Table 6.3 in the Appendices, including the volumes of water necessary for deposition of the minimum and maximum volumes of evaporites.

In Figure 3.3 it can be seen that the amount of water necessary for deposition of the carbonates is the highest, with an average water column of ~400 km for the Z2 Carbonate (provided the carbonate is deposited as an evaporate). The gypsum deposits require significantly less water and the halite deposits requires the least amount of water, e.g. the Z1 Halite only requires 92 m of water on average.

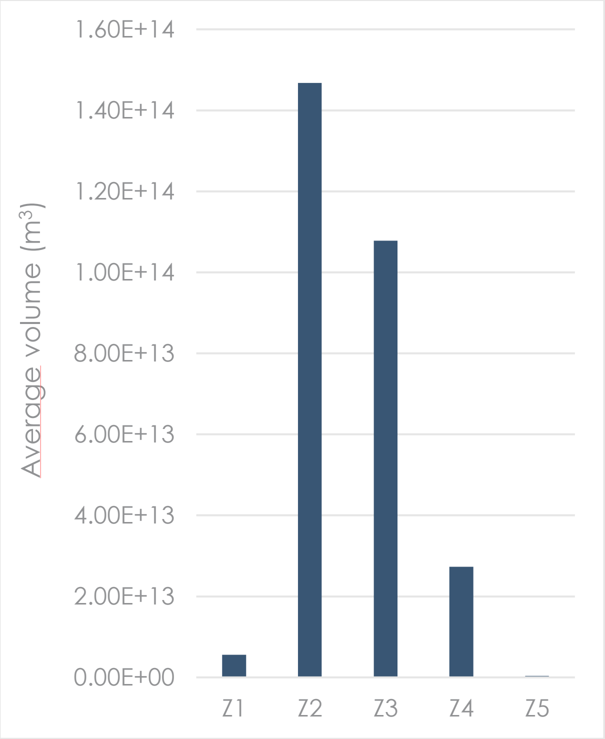

Figure 3.1. Average volumes of the different Zechstein cycles.

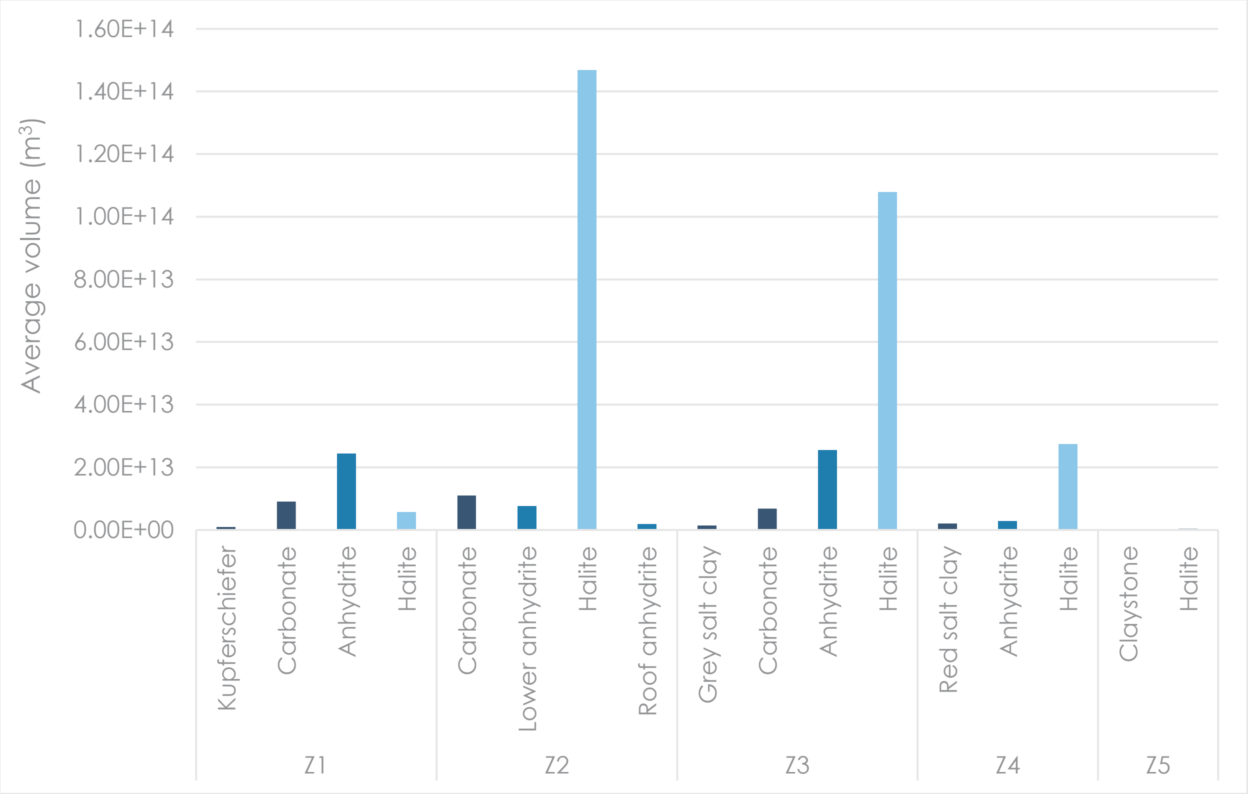

Figure 3.2. Average volumes of the different Zechstein sediments, sorted per Zechstein cycle. The volumes of the Z5 deposits are too insignificant to be able to be seen in this graph.

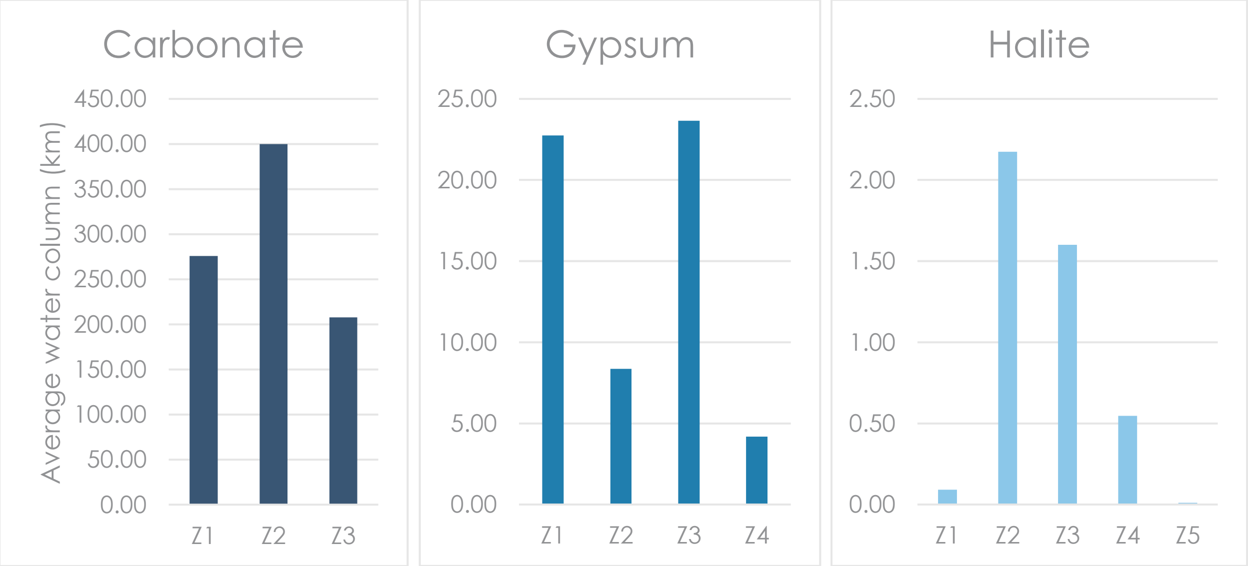

Figure 3.3. The average water column necessary for deposition of each of the average volumes of the Zechstein evaporites, deposits from a basin that has the concentration at saturated of the relevant evaporite. On the x-axis the Zechstein cycles can be found. Note that the scale on the y-axis is different for each of the three types of deposits.

3.3 Duration of deposition

The duration of deposition for the average volumes of the Zechstein evaporites is given plotted in Figure 3.4, assuming an evaporation rate of 2 m/yr. This evaporation rate is a good modern-day analogue for the location of the SPB during the deposition of the Zechstein.

All the data is summarized in Table 6.4 in the Appendices. The total calculated duration of deposition for the average size of the deposits is 560.000 yr, with a duration for the minimum and maximum size of deposits of 285.000 yr and 1.04 Myr. The carbonates take longest to deposit and the halite can be precipitated in an even shorter amount of time. No clear trend, e.g. the evaporite of each next cycle takes less time to form, can be observed. The values for the carbonate are only valid if the carbonate is deposited as an evaporite and/or building blocks for the carbonate are only brought into the basin through a marine influx.

The calculated net evaporation rate is given in Table 3.2 and is calculated for both the slow and fast deposition rates for the gypsum and halite (using Equation 2.10c, see Section 2.2). It demonstrates that a faster deposition rate requires a faster evaporation rate.

Table 3.2. Calculated evaporation rate for both a slow and a fast deposition rate.

	Slow deposition rate (m/yr)	Fast deposition rate (m/yr)
Gypsum	1.52	15.16
Halite	3.38	10.15

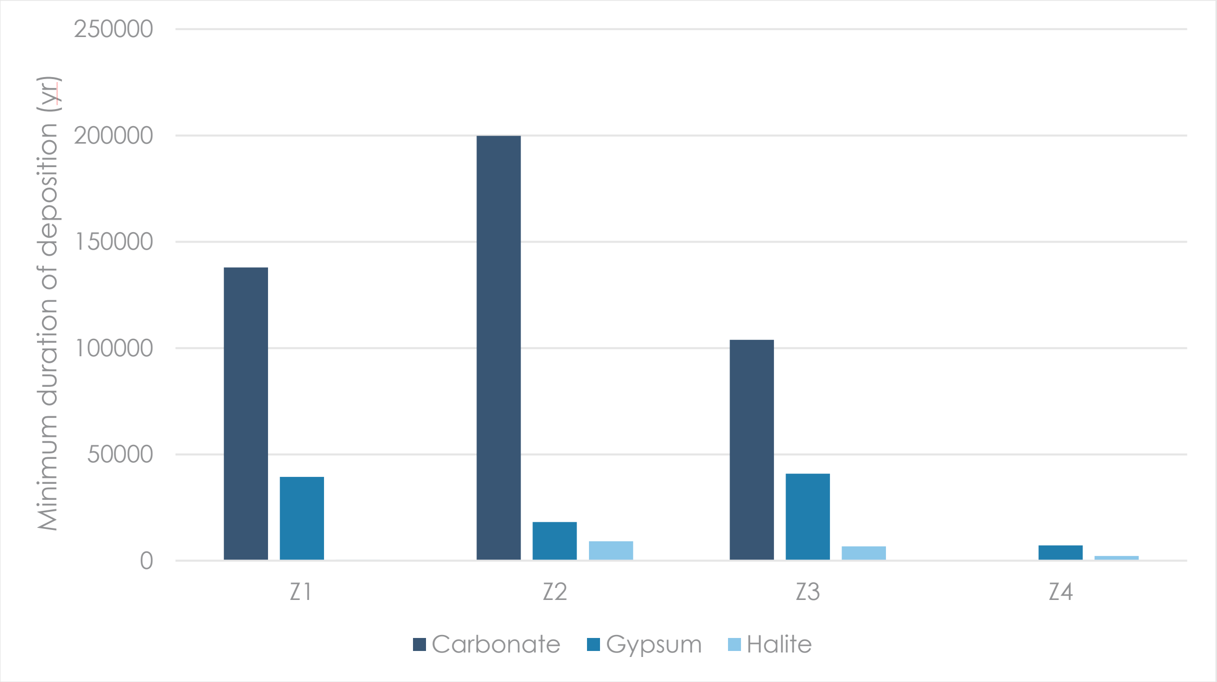

Figure 3.4. Minimum duration of deposition for the average volumes of the Zechstein evaporites.

The calculated deposition rate for the gypsum and halite (using Equation 2.14, see in Section 2.2) is given in table 3.3, for a net evaporation rate of 2 m/yr.

Table 3.3. Calculated deposition rate for an evaporation rate of 2 m/yr.

	Deposition rate (m/yr)	Deposition rate (mm/yr)
Gypsum	0.00132	1.32
Halite	0.02954	29.54

The influxes of water from an oceanic realm into the basin are given per cycle in Table 6.5 in the Appendices, as these are proportional to the surface area of the basin/sediments.

3.3.1 Duration until saturation is reached

If there was only an influx of water into the basin, the amount of time during which carbonate was the only mineral to precipitate and during which gypsum was the only mineral to precipitate are given in Table 3.4 for a variety of water depths. It is assumed that the average water depth during the deposition of each Zechstein cycle is the same. It can be seen that the timespan during which carbonate is the only to precipitate and during which gypsum is the only mineral to precipitate are really short. Most likely an outflow must thus have been present.

Table 3.4. Amount of time during which carbonate/gypsum is the only mineral to deposit in the SPB.

Average water depth in the basin (m)	Time during which carbonate is the only mineral to precipitate (yr)	Time during which gypsum is the only mineral to precipitate (yr)
100	128	254
200	256	508
300	383	762
400	511	1016
500	639	1270
600	767	1524

3.4 Accommodation space in the basin

A cross-section in the offshore Netherlands has been constructed trough the Zechstein in order to investigate the variations in accommodation space in the basin. The location of the cross-section is given in Figure 6.8 (see the Appendices) and the cross-section is given in Figure 6.10 (see the Appendices), with the Z1 individually presented in Figure 3.5 with the locations of the pseudo wells. All data used for the construction of this cross section is summarized in Table 6.6 in the Appendices.

The cross section through the Z1 shows relatively homogenous thicknesses of the Kupferschiefer and of the carbonate and anhydrite towards the north. In the southern part of the cross section both the anhydrite and carbonate are thicker compared to the north, with the anhydrite having a significantly greater thickness. The halite is only limitedly present in this cross section and the thickest part of the halite is present where the anhydrite is also the thickest. In Well 1 no halite is present, all the other sediments are present in all the wells.

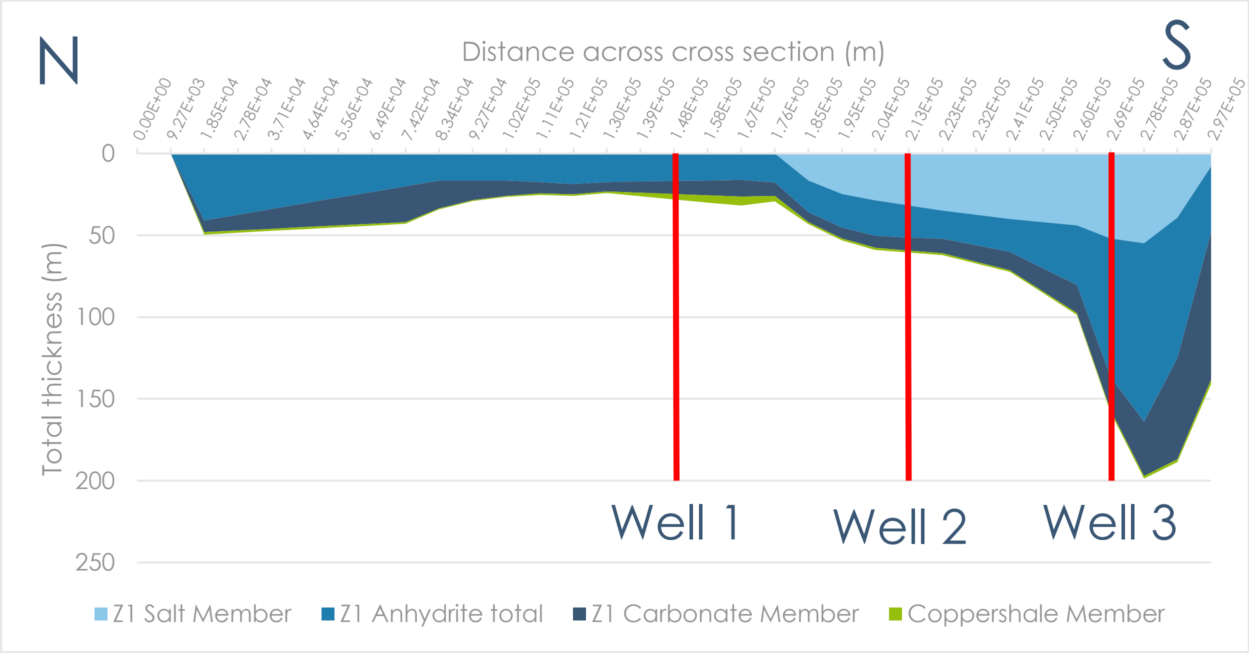

Figure 3.5. Cross section as found in Figure 6.10, with the locations of the three pseudo-wells

The thickness in each well over time is plotted in Figure 3.6, where the slope of the curve represents the sedimentation rate and thus indicates how fast the accommodation space is filled. This plot shows a quite uniform, but slightly increasing, sedimentation rate during the deposition of the carbonates in Well 1 and 2, while there is a minor increase during the deposition of the carbonate in Well 3. During the deposition of the anhydrite in Well 1 and 2 the sedimentation rate increases slightly, while this increases more in Well 3. During the deposition of the halite in Well 2 and 3 there is a substantial increase in the sedimentation rate. No halite is present in Well 1 and thus such an increase is not present.

To find out what the amount of accommodation space was and how this was filled, the parameters that influence the slope of this curve need to be investigated. As discussed earlier on, the slope is influenced

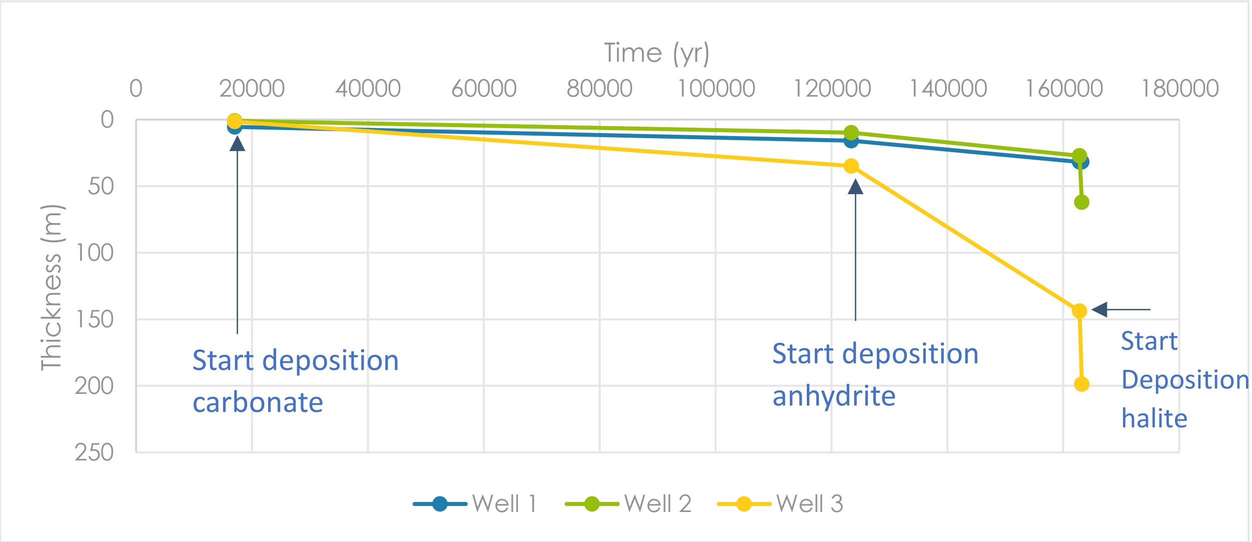

Figure 3.6. Thickness over time for the cross section in Figure 3.5. Start of the deposition of the carbonate, anhydrite and halite is annotated. Data can be found in Table 6.7 in the Appendices.

by eustatic sea-level changes, isostatic or tectonic subsidence or could suggest that the basin has been (partly) filled.

Eustatic sea-level changes are ignored, as discussed in the Method (see Section 2.4), and the vertical response due to isostatic subsidence can be calculated.

The plot is adjusted for the vertical response as predicted by the isostatic balance in Figure 3.7, all data is summarized in Table 6.8 in the Appendices. The first thing that can be noted in this plot is that the total thickness in all wells has decreased. The thickness of the carbonates is additionally in the same range in all wells, on the contrary what can be seen in the non-adjusted plot (Figure 3.6). There are however still some changes in the slope of the curves that cannot be explained by the isostatic balance, which are as following:

- Slight overall increase during the deposition of the carbonates
- Small increase during the deposition of the anhydrite in Well 1 and 2
- Significant increase during the deposition of the anhydrite in Well 3
- Significant increase during the deposition of the halite in Well 2 and 3

There are a few possible explanations for this. It could be the case that the basin is (partly) filled up and that the accommodation space thus (partly) decreases. Another possibility could that be a tectonic subsidence component plays a role and that the accommodation space thus increases or stays the same. The last reason could be that there is that the effect of eustatic sea-level changes is too significant to be ignored. These options are investigated in the discussion (see Section 4.3).

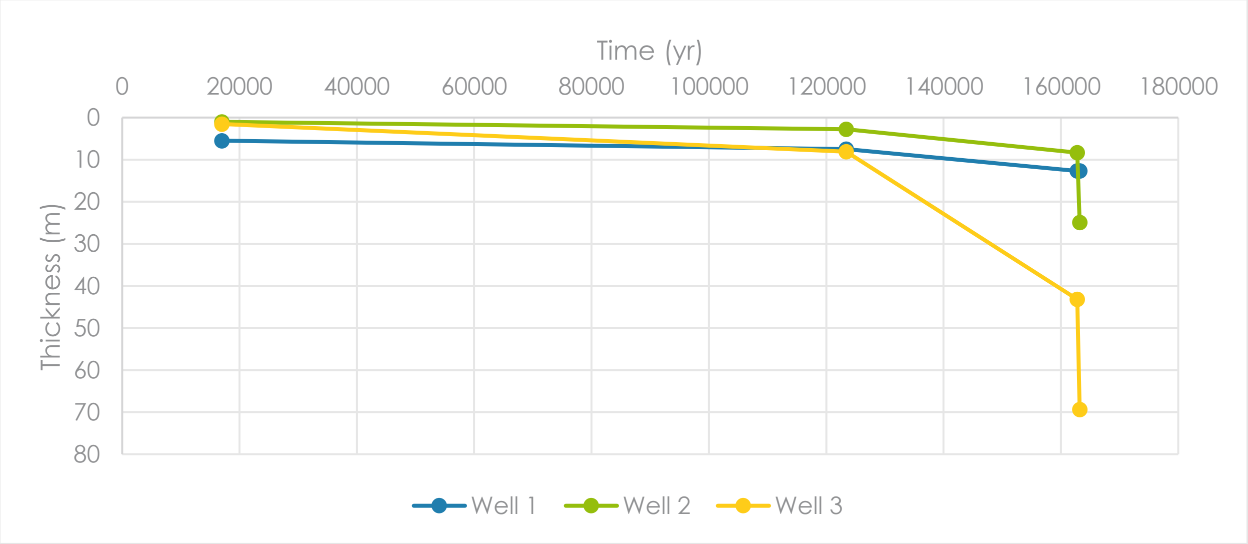

Figure 3.7. The thickness over time from Figure 3.6 adjusted for the vertical response due to the isostatic balance. Data can be found in Table 6.8 in the Appendices.

4 Discussion

4.1 Assumptions and uncertainties

Within the quantitative analysis presented in this report there are a few assumptions and uncertainties present. They are listed below and afterwards discussed in more detail. The assumptions include the following:

- The evaporation rate of 2 m/yr
- The delivery of building blocks towards the Zechstein sediments only happens through the connection with a marine realm
- The surface areas of the Zechstein deposits
- The surface area of the Zechstein deposits is equal to the surface area of the Southern Permian Sea and the volume of water in the basin stays constant and the
- For several of the calculations all the anhydrite is expected to have originally been deposited as gypsum

The uncertainties lie within the range of the volumes of the Zechstein deposits and the method that is used for their calculation.

4.1.1 Assumptions

For the location of the SPB during the deposition of the Zechstein an evaporation rate of 2 m/yr has been assumed. A lot of the calculations hinge on this value and thus this assumption is rather important. However, for the location of the SPB (paleolatitude of ~20° N) and the arid climate (Geluk, 2005), a value of 2 m/yr is on the higher end of oceans nowadays around that latitude (Babkin, 2009) and thus quite reasonable considering the basin is more isolated than an ocean.

The delivery of all building blocks necessary for the Zechstein sediments is assumed to only happen through a connection with a marine realm, where the input of water and building blocks from run-off and rainfall are thus ignored. This is actually fairly justifiable, as the arid climate would also have been responsible for low precipitation rates (Legler et al., 2005). At least, this is the case for the gypsums and halites, as the contribution of building blocks in the water from run-off would be insignificant compared to the amount of building blocks coming from a marine connection. This is not exactly the case for the carbonates, as these are biogenic and not evaporitic and the process by which they are deposited thus differs from the evaporites. It can therefore not be determined with certainty (or at least not within the scope of this report) that all building blocks necessary for the deposition for the carbonates are delivered by a connection with an ocean. All calculations regarding the volumes of water necessary for deposition and the duration of deposition regarding the carbonates are consequently not that meaningful. Nonetheless, they still give some indication or rough ideas regarding these parameters and should not be disregarded completely.

Another assumption lies within the surface areas of the Zechstein deposits. For the Z1, Z2 and Z3 Carbonates the surface area from the distribution and thickness maps as found today from Peryt et al. (2010) are used. Such maps are not available for the other sediments in these cycles and thus the same surface areas are used for the other sediments in these cycles. For sediments in the Z4 and Z5 cycles the same surface areas are used for the clays, gypsums and halites as given in the distribution maps from Peryt et al. (2010).

These same surface areas are used as the surface area of the Southern Permian Sea, as no other information is known regarding this surface area and it is thus considered to be the best approach. Furthermore, the volumes of water in the basin are assumed to be constant in some of the calculations (see Section 2.3).

Lastly in the water volume, the duration of deposition and the duration until saturation is reached calculations (see Section 2.2 and 2.3) the assumption is made that all the anhydrite present in the subsurface was originally deposited as gypsum. A decrease in volume is associated with these different types of sulfates and gypsum also has a different density than anhydrite (2200-2400 kg/m^3 vs. 2900-3000 kg/m^3; Van den Belt & de Boer, 2007). In reality the deposition of anhydrite and gypsum is bound by conditions such as water depth and temperature, but gypsum is very easily converted to anhydrite by dehydration (Warren, 2016). It is very likely that most of the anhydrite found in the subsurface today was actually deposited as gypsum. However, it is difficult to determine where and if this is the case within the scope of this research. It is thus assumed for the volume calculations and such that the anhydrite was deposited as gypsum. In the calculations using the isostatic balance (see Sections 2.4.1.2 and 3.4) the distinction between anhydrite and gypsum is necessary to make, as there is a difference in density between these sulfates. It is assumed that anhydrite is mostly deposited on the platform and that gypsum is deposited on the slope of the platform (Van den Belt & de Boer, 2007)

4.1.2 Uncertainties

The volume calculations for the Zechstein sediments can be characterized by large uncertainty values. First of all, for most formations a certain amount of the deposits has been eroded away undeniably, but it is difficult to account for this. This will thus not be discussed further. Secondly, for all the volume calculations minima, maxima and average volumes are given. However, all conclusions in this report are based on the average volumes and might thus not be completely correct or do not represent the results wholly accurately. Using the average volumes is nonetheless the best approach possible, but it should be kept in mind when conclusions are made that these volumes are the average.

Other uncertainties lie within the method that is used to calculate the volumes of the different formations. The volumes that have been calculated using the distribution maps from Peryt et al. (2010) cannot be calculated more accurately and its uncertainties cannot be lowered. The question may however arise if the methods used to calculate the volumes of the formations using well top data from the offshore Netherlands is correct. It is likely that the way in which the deposits are found in the offshore Netherlands are not representative of the whole SPB and extrapolating from the offshore Netherlands might result in a distorted calculation. It can however be checked how accurate these methods are, as the same method can be applied to formations of which the volumes from the distribution and thickness maps from Peryt et al. (2010). This has been done for the Z1, Z2 and Z3 Carbonates, of which the results can be found in Table 6.2 in the Appendices. The average volume of the carbonates is only 6-8% off the volumes from the distribution and thickness maps from Peryt et al. (2010), while the minimum and maximum volumes are significantly more off.

The last uncertainty lies in the volumes of the Z5 sediments. The occurrence of these sediments is very limited in the Netherlands, which reflects a shift of the depocenter of the basin more towards the East (De Jager et al., 2007). Their thicknesses as presented in this report do thus not reflect the full extent of their occurrence in the whole SPB. This cycle is more or less ignored for the remainder of this report.

4.2 Connection to oceanic conditions

Based on current water volume estimates it can be concluded that there must have been a constant (or almost) connection to a marine realm during the deposition of both the carbonates and gypsums, as the average water column that is necessary for deposition of these (average volumes) deposits is 5 km as a minimum (Z4 gypsum) up to 400 km (Z2 carbonate). The basin is believed to not have been deeper than 300 m (Peryt et al., 2010 and reference therein) and water depths of 5 km of more seems thus very unreasonable. Even several floodings would not provide enough input material for deposition of the evaporites. It must be noted again that in these water volume calculations might not be correct for the deposition of the carbonates, as these are biogenic, but it still gives a rough indication of the water volumes necessary for deposition.

The situation for the halite is a bit different. The Z1 Halite only requires an average water depth of ~92 m, which seems a very reasonable number. The Z2, Z3 and Z4 Halites require a bit more water, but this can either be accomplished by several floodings or a constant connection to a marine source.

4.2.1 Size of and fluxes in the strait

The question may arise how large the connection to the sea, thus the straight connecting the basin to the sea, must have been. This can fairly easily be done by comparing the fluxes in the basin to fluxes in other basins, such as the Mediterranean sea.

For easier comparison, the influxes as presented in Section 3.3 are also given in sv (1 sv = 10^6 m^3/s; Meijer, 2006) in Table 4.1. Two present-day possible analogues are the Strait of Gibraltar and the strait of Sicily. The Strait of Gibraltar has a flux of 0.8-1.6 sv (Meijer et al., 2004) and has dimensions of 300 m by 12 km (Lacombe and Richez, 1982). The strait of Sicily has a flux between 0.8 and 1.4 sv and a depth of 300 m (Meijer, 2006). The smallest flux for the SPB is ~0.04 sv (see Table 4.1), suggesting that size of the strait that allows oceanic water into the SPB only needs to be 20 times as small as the Strait of Gibraltar. This does not necessarily indicate that the strait was that small, but a large strait is not required to bring the amount of water needed for deposition of the Zechstein deposits. This is the case if there is only a flux of water into the basin

There is however reason to believe that the strait to the sea was larger than indicated by only the influx of water as given above, as an outflux of water from the basin to the ocean is necessary as well during the deposition of the carbonates and gypsums and this is not accounted for yet.

Table 4.1. Fluxes of water into the basin in sv (106 m3/s). The fluxes are split out into the carbonates and gypsums and the halite, as the fluxes are dependent on the surface areas and the surface areas of the halites are different from the carbonates and gypsums.

Carbonate and gypsum		Halite	
Cycle	Fluxes (sv)	Cycle	Fluxes (sv)
Z1	0.0413	Z1	0.0313
Z2	0.0349	Z2	0.0347
Z3	0.0416	Z3	0.0346
Z4	0.0256	Z4	0.0256
		Z5	0.0152

The reason why an outflux is required additionally, is that the time it takes for the basin to reach gypsum saturation (383 yr for a basin depth of 300 m) in a basin in which carbonate is deposited, is significantly shorter than the time it takes to form the carbonates (100-200 kyr for the Z1, Z2 and Z3 Carbonates). Even though these calculations might not be completely correct for the biogenic carbonates, the difference between the time it takes for the carbonate to form and the time it takes for the basin to reach the gypsum saturation is too significant to be explained by another process of deposition for the carbonates.

A flux out of the basin is also required during the deposition of the gypsum, as there is again a large difference between the time it takes for the basin to reach halite saturation (762 yr for a basin depth of 300 m) during the deposition of gypsum, which takes about 18-40 kyr.

From this it can be concluded that during the deposition of both the carbonates and gypsums and outflow of water must also have been present. This also fits with earlier conclusions regarding a constant connection to marine circumstances during carbonate and gypsum precipitation.

4.2.1.1 Calculation of outflux in the basin during gypsum precipitation

The size of the outflux can be calculated during the gypsum precipitation, as an outflux is necessary during the deposition of the gypsum. This is also required during the deposition of the carbonate, but as the process by which the carbonate is deposited differs from the gypsum and halite this cannot be concluded with absolute certainty. For the halite no outflux from the basin is necessary and there is thus no need for a calculation for the size of the outflux.

The simple model as presented in Figure 2.1 in the Method is adjusted by the addition of an outflux and the addition of the deposition rate. The adjusted model can be found in Figure 4.1. There is a water balance in the basin as described by Equation 4.1:

$$[4.1]\ Q_0 = Q_b + e \cdot A$$

Q_0 = volume (in)flux of ocean water (m^3/yr)
Q_b = volume (out)flux of water from the SPB (m^3/yr)
e = rate of net evaporation (m/yr)
A = surface area of the basin (m^2)

There is also a total salt balance as described by Equation 4.2:

$$[4.2]\ Q_0 \cdot S = Q_b \cdot S_b + d \cdot A \cdot \rho$$

S = total salt concentration of Permian seawater (kg/m^3)
S_b = total salt concentration in the SPB (kg/m^3)
d = deposition rate (m/yr)
ρ = density of gypsum (kg/yr)

The total salt concentration in the basin is equal to the saturation concentration of gypsum (145 kg/m^3) and does not change over time. Combining Equation 4.1 and 4.2 links the influx to the evaporation rate and the deposition rate. This is described by Equation 4.3a:

$$[4.3a]\ Q_b \cdot S_0 + e \cdot A \cdot S_0 = Q_b \cdot S_b + d \cdot A \cdot \rho$$
$$e \cdot A \cdot S_0 = Q_b \cdot (S_b - S_0) + d \cdot A \cdot \rho$$

Which can either be rewritten to calculate the evaporation rate, as described by Equation 4.3b, or the deposition rate, as described by Equation 4.3c:

$$[4.3b]\ e = (Q_b \cdot (S_b - S_0))/(A \cdot S_0) + (d \cdot \rho)/(e \cdot S_0)$$

$$[4.3c]\ d = (e \cdot S_0)/\rho - (Q_b \cdot (S_b - S_0))/(A \cdot \rho)$$

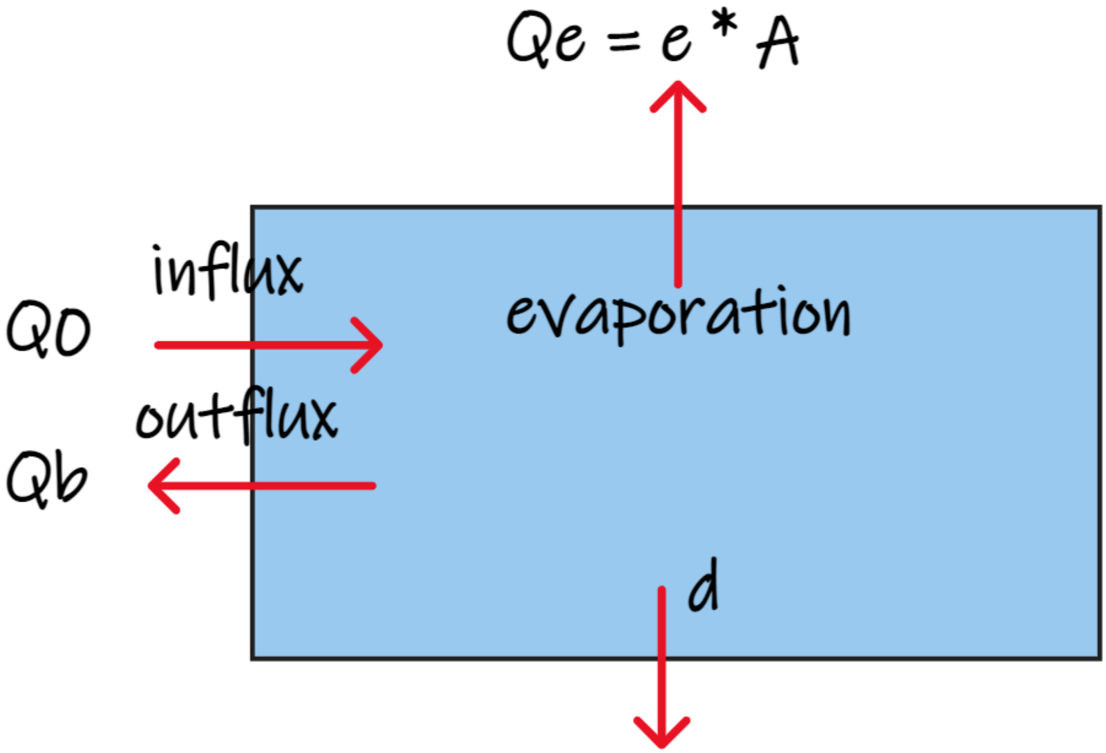

Figure 4.1. Simple model similar to the model presented in Figure 2.1, but adjusted for by the addition of an outflux for the deposition of the gypsum. All the equations and parameters are described in Equation 4.1, 4.2 and 4.3.

Equation 4.3c can be plotted using the Python script given in Section 6.1 in the Appendices for different relations between the evaporation rate and the outflux. The result is plotted in Figure 4.2, showing the relationship between the rate of net evaporation over the rates of deposition for the gypsum for different amounts of the outflux. As the assumed net evaporation rate is 2 m/yr and the deposition rate of gypsum is 1-10 mm/yr (see Table 2.3), the expected outflux in the basin would be $0.4 \cdot e \cdot A$. This is not necessarily something that can be used in this report to further discuss the dynamics in the basin, but it can be quite useful if the dynamics during the deposition of the Zechstein are further modeled.

Equation 4.3b also indicates that if the outflow is ignored, the net evaporation rate is underestimated. The opposite can be said regarding Equation 4.3c: if the outflow is ignored, the deposition rate is overestimated. Figure 4.2 furthermore shows that there is a linear relation between the deposition rate and the net evaporation rate, which has also been found in the Results (see Section 2.3).

4.2.2 Check of duration of deposition

The implications of the duration of deposition for the model of the basin with only an influx as presented in Section 3.3 has been shortly discussed before in this section, but these durations have not yet been compared to known durations of the Zechstein.

It must be noted again that these duration calculations are based on an assumed evaporation rate of 2 m/yr, on the assumption that all building blocks for the deposition of the Zechstein are delivered from a marine source and on the assumption that there is no outflux present. It has already been discussed that the evaporation rate is quite a good analogue for the paleo-location of the Zechstein, but there is no

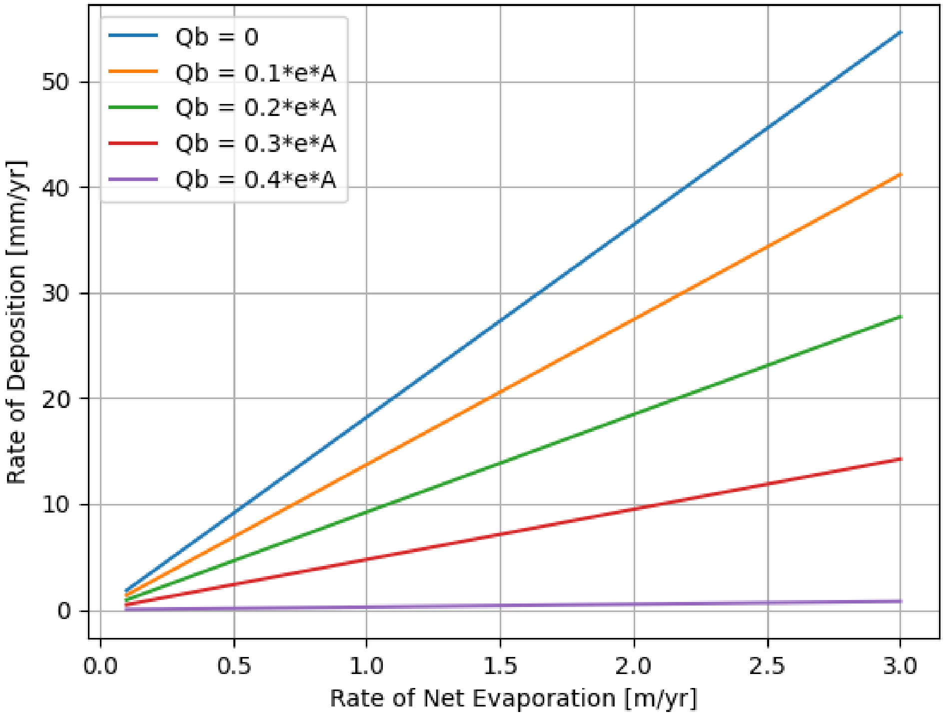

Figure 4.2. The relationship between the rate of net evaporation and the rate of deposition for gypsum for different amounts of outflux, in a situation where there is both an in- and outflux in the SPB. The script used to construct this figure can be found in Section 6.1 in the Appendices.

certainty on how the building blocks for the carbonates are delivered and moreover, it has been found that there must have been an outflux during the deposition of the carbonates and the gypsums. This makes this whole comparison not that reliable, but an attempt will still be made to do so. If it would be the case that the durations of the cycles would exceed the established durations or that the total calculated duration of the Zechstein would surpass the total established duration of the Zechstein, then the case could be made that the models used in this research are not trustworthy at all. Nevertheless, no further conclusions can be made based on these comparisons.

The longest calculated duration is 1.04 Myr, for the maximum volumes of the deposits. This fits with the total duration of the Zechstein, estimated to be approximately 6 Myr (Schneider and Scholze, 2018). There are no known estimates regarding the duration of deposition of each individual Zechstein deposit, but estimates regarding the duration of each cycle are established by Menning et al. (2005). These durations are presented in Table 4.2 and compared to the calculated total duration for the minimum, maximum and average volumes of the Zechstein deposits. In this table it can be seen that none of the calculated durations exceed the established duration as presented by Menning et al. (2005).

From these comparisons no significant conclusions can be made. The calculated durations do not surpass the established durations, in which case the calculations would be completely untrustworthy, but this not the case.

Table 4.2. Comparison between established and calculated duration of the Zechstein cycles.

Cycle	*Established approximate duration (Myr; Menning et al., 2005)*	Calculation total duration (see Table 6.4)		
		Minimum volume (yr)	*Maximum volume (yr)*	*Average volume (yr)*
Z1	2	84,979	331,994	177,643
Z2	0.8	137,024	386,324	227,065
Z3	0.8	61,491	294,692	151,547
Z4	0.2 - 0.4	1,641	26,729	9,536
Z5	0.1	38	57	47

4.3 Basin dimensions and dynamics

As discussed in the Results, the basin architecture and dynamics are investigated by looking at the accommodation space in the basin. In order to examine this accommodation space a cross-section in the offshore Netherlands has been constructed trough the Z1 cycle. Within this cross-section three pseudo-wells have been constructed to inspect the evolution of the accommodation space in each well over time. The thickness over time in each well has been plotted in Figure 3.7 where the slope of the curve represents the sedimentation rate. This curve is influence by the eustatic sea-level changes, isostatic or tectonic subsidence or by the (partly) filling of the basin. The curve has already been adjusted for the vertical response as predicted by the isostatic balance in Figure 3.7. There are however still some changes in the slope of the curves that cannot be explained by the isostatic balance, which are as following:

- Slight overall increase during the deposition of the carbonates
- Small increase during the deposition of the anhydrite in Well 1 and 2
- Significant increase during the deposition of the anhydrite in Well 3
- Significant increase during the deposition of the halite in Well 2 and 3

These changes can either be explained by tectonic subsidence, changing sea-levels or the (partly) filling of the basin).

The change in sea-level is difficult to incorporate in this curve. Even though on a large scale the sea-level fell down during the Late Permian (Haq & Schutter, 2008), smaller fluctuations of the sea-level have been found in the Zechstein deposits (Peryt et al., 2010 and reference therein). Including this is thus quite difficult and unfortunately does not completely fit within the scope of this project. The effects of sea-level fluctuations are thus ignored for now.

The tectonic subsidence in the case of the Zechstein is generally due to thermal relaxation of the crust (Van Wees et al 2000, Peryt et al., 2010). It can be assumed that at least a significant the amount of tectonic subsidence during the Late Permian was rather constant and slow. This is not what has been found in the subsidence curves by Van Wees et al. (2000), as can be seen in Figure 4.3. Tectonic subsidence also varies across different regions in the SPB, mostly because of different underlying structures in the basin (Van Wees et al., 2000). However, Figure 4.3 does seem to indicate that during the beginning of the Late Permian the tectonic subsidence is increasing constantly and thus the assumption that the amount of tectonic subsidence was constant during the deposition of the Z1 seems to be valid. As this tectonic subsidence is expected to be slow, it could be estimated that this rate is somewhat equal to the slight overall increase in the thickness over time during the deposition of the carbonates.

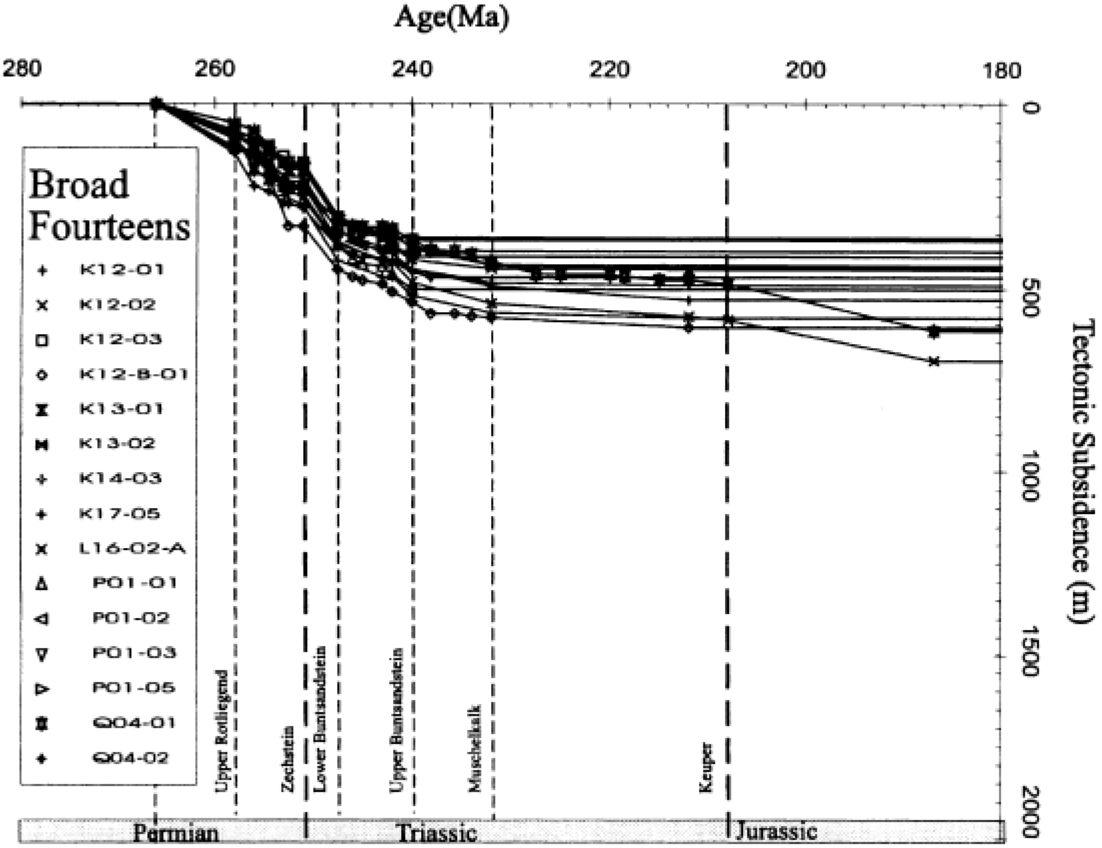

Figure 4.3. Air loaded subsidence for the Broad Fourteens Basin in the offshore Netherlands. The tectonic subsidence has already been corrected for isostasy. This graph indicates significant, stepwise, tectonic subsidence during the deposition of the Late Permian. Adapted after Van Wees et al. (2000).

The remainder of the change in slope of the curve (see Figure 3.7) that has yet to be explained is the increase during the deposition of the anhydrite and halite. There are two possibilities that can explain this, either there is another tectonic component such as faulting (and there is an increase of the accommodation space), or the basin is (partly) filled up (and therefore is a decrease of the accommodation space towards zero).

It is at least certain that faulting plays a role, as syn-tectonic faulting took place during the deposition of the Z1 Anhydrite. This created more accommodation space in the basin, which was subsequently filled by both more anhydrite and the halite (Geluk, 1999; Geluk, 2005). This could also explain the very limited distribution of the Z1 Halite. This syn-tectonic faulting would have locally made the basin deeper during the anhydrite precipitation, allowing the halite to be locally precipitate in this deeper part of the basin.

No information regarding the exact amount of offset along these fault planes is given in the literature, but it seems logical that this tectonic exponent could at least partly explain the increase in accommodation space during the deposition of the anhydrite and halite as seen in Figure 3.7. It can however thus not be determined with absolute certainty how large the effect of this faulting is on the creation of accommodation space for the anhydrite and halite. This also would suggest that the remainder portion of the change in slope of the curve is explained by the filling of the basin with sediments, although it is thus not certain how significant the impact of this is.

What can be established with certainty is that at the end of the deposition of the anhydrite the basin could not have been completely filled up, as then there would have been no water with the correct salinity to provide material input to precipitation of the halite series. It could have very well been the case that after the deposition of the Z1 Halite the basin was completely filled or no more water was present, as precipitation of the halite would otherwise have then continued. Either way, this implies that at the end of the Zechstein 1 cycle the whole accommodation space was filled.

4.3.1 Timing of isostatic subsidence

One major factor that has not been considered is the timing of the isostatic subsidence, and possible delayed response due to loading. In the curves presented in Figure 3.7 and the discussion of the accommodation space that is necessary for this curve it has not only been assumed that isostatic subsidence is a syn-depositional process, but also that the vertical response as predicted by the isostatic balance works on the same timescale as the deposition of the deposition of the evaporates. The isostatic response time is around 10 kyr (Watts, 2001, as cited in Van den Belt & de Boer, 2007) and thus works on the same timescale as the deposition of the anhydrite/gypsum (deposition time of > 10 kyr, see 6.4), but not on the same timescale as the precipitation of the halite. The Z1 Halite can be deposited in 383 years, which nowhere near the response time of isostasy. The vertical response due to the load of the Z1 Halite would therefore take place long after the halite is deposited. This delayed subsidence would thus cause deepening of the basin, creating the accommodation space for the next cycle. Moreover, tectonic subsidence also continues and this also contributes to the further subsidence of the basin.

After the deposition of the Z1 cycle the basin will at some point have subsided enough for it to flood, filling it with water and start the deposition of the next cycle. The flooding of the basin will also create more subsidence, as the (sea)water will also exert a load on the crust. Isostasy equations from Van den Belt & de Boer (2007) can be amended for a situation where a dry basin is flooded and subsides, as described by Equation 4.1:

$$[4.1]\ D_{basin\_dry} = ((\rho_{asthenosphere} - \rho_{water})/(\rho_{asthenosphere} - \rho_{air}) \cdot D_{basin} = 0.7 \cdot D_{basin}$$

D_{basin_dry} = the depth of the basin without water (m)
ρ_{air} = the density of air (kg/m^3)

If this equation is applied to the basin depth at the start of the Zechstein, it is found that the original basin depth of the Zechstein only had to be 140-210 m, as water depth during the deposition of the Kupferschiefer have been estimated to have been 200-300 m (Van Wees et al., 2000).

4.3.2 Cyclicity in the Zechstein sediments

The newly created accommodation space after the deposition of the Z1 cycle allows for deposition of the next Zechstein cycle, after which the same process as described above can occur. The basin is filled with the a claystone, carbonates, gypsum and halite, and the delayed isostatic subsidence together with the tectonic subsidence allows for the creation of new accommodation space after the Zechstein cycle has been deposited. This delayed isostatic response thus contributes significantly to the formation of the cyclicty in the Zechstein sediments.

It seems that from the Z2 cycle onwards, the volumes of the Zechstein deposits in the various cycles have increasingly gotten smaller, implying that the basin has filled up and the total amount of accommodation space has decreased with each cycle. Another factor that could play a role in this is that the topography of the Z2 cycle was somewhat different compared to the other cycles. The basin just before the deposition of the Z2 Carbonates was most likely deeper compared to other cycles, as turbidites with a Bouma sequence (or at least significant parts of Bouma sequences) have been identified in the slope deposits of the Z2 Carbonate in North-East England (Mawson and Tucker, 2009), in North-East Germany (Kaiser et al., 2003) and in Poland (Jaworowski and Mikalajewski, 2007). The presence of turbidites suggests a steeper slope. Turbidites have not been found in the Z1 and Z3 Carbonates, suggesting that the basin was deeper at the start of the Z2 Carbonate compared the other cycles.

It has been suggested that the pre-existing topography of the Z1 Anhydrite influenced this steep slope in the Z2 Carbonate (Kaiser et al., 2003; Geluk, 2005). A possible cause for this could lie in the syn-tectonic faulting during the deposition of the Z1 Anhydrite in combination with the very localized deposition of the Z1 Halite. This would have caused a delayed isostatic reaction (as discussed above), locally deepening the basin after deposition had ended, and creating a steeper slope for the deposition of the Z2 cycle.

After the deposition of the Z2 Halite the relief of the basin was mostly filled, as indicated by the occurrence of potassium-magnesium salts at the top of the Z2 Halite (Geluk, 2005). This would also explain why there is no steep slope in the Z3 and later Zechstein cycles. Furthermore, this could also possibly play a role in the decreasing size of the deposits of the later Zechstein cycles, as there is simply less relief and a shallower basin.

From the Z4 cycle and further onwards no more carbonates are present, suggesting that fully marine conditions were not present in the basin from that point onwards, as no more carbonates are present in the Z4 and Z5 cycles (Geluk, 2000; Geluk, 2005; Peryt et al., 2010). A cause for this could possibly be a very restricted inflow of water, which does not allow the water in the basin to stay within the salinities in which carbonates are formed.

It however remains uncertain whether the rates used for isostatic and tectonic subsidence are realistic. Furthermore, the calculations and conclusions described above have only been tested on the Z1 cycle in the subsurface of the Netherlands. It is thus unclear whether this would also work on the later cycles and if it would also work for the whole SPB. The answers to this unfortunately do not lie within the scope of this study and would be great questions for further research, in which the construction of complete 3D basin model would be most useful.

4.4 Basin model

The question remains what this implies for the type of basin in which the Zechstein was deposited based on the assumptions named in Section 4.1.1 and the syn-depositional vertical response as predicted by the isostatic balance.

It has been suggested that the basin in which the Zechstein was deposited was characterized by the shallower water-deep basin model origin, due to its thick evaporite deposits (Van den Belt & de Boer, 2007 and reference therein). Only if isostatic compensation is considered to be a simultaneous process with the deposition of the evaporites, such a basin is not needed and a shallower water-shallow basin model will provide the necessary accommodation space for the Zechstein. There is however a delayed isostatic response for the precipitation of the halite series, but multiple phases of halite precipitation remove the need for a deeper basin (Van den Belt & de Boer, 2007). This is at least the case for the Z2 Halite, which has been deposited in three phases (De Jager et al., 2007).

The shallower water-deep basin model is not completely ruled out by this, but it just is not necessary for the deposition of these thick deposits (Van den Belt & de Boer, 2007). However, the shallower water-deep basin model seems unlikely for the deposition of the Zechstein for another reason. In this model the basin is located significantly lower than the sea and water inflow into the basin happens due to periodic overflow, seepage and continental groundwater inflow (Warren, 2016). Due to the large volumes of water and long durations necessary for the deposition of carbonates and anhydrites a constant connection to marine conditions had to be established. This is simply not possible in the shallower water-deep basin model and thus this model seems even more unlikely compared to the shallower water-shallow basin model.

5 Conclusion

The goal of this internship was to improve our understanding of the basin architecture and dynamics of the Southern Permian Basin during the deposition of the Zechstein. It was investigated how the SPB may have developed during deposition of the Zechstein.

The most important conclusions are that:

- There was a constant connection to a marine realm during the deposition of the carbonates and anhydrites. This connection was not necessary for the deposition of the halites.
- The cyclicity within the Zechstein deposits can be explained by variations in the isostatic balance, to which the delayed isostatic response after the fast deposition of the halite contributes significantly.
- The basin in which the Zechstein was deposited could be similar to a shallower water-shallow basin model.

The question remains whether these findings are applicable to the whole SPB and if the isostatic and tectonic subsidence rates are realistic. The construction of a complete 3D basin model would be most fruitful in order to investigate these questions.

Other unanswered question are by which processes the carbonate is exactly deposited, what the influence of eustatic sea-level variations exactly and how significant these are, and what the actual size of the connection with the ocean is.

References

Azam, S. (2007). Study on the geological and engineering aspects of anhydrite/gypsum transition in the Arabian Gulf coastal deposits. *Bulletin of Engineering Geology and the Environment*, *66*(2), 177–185. https://doi.org/10.1007/s10064-006-0053-2

Babkin, V. I. "Evaporation from the surface of the globe." *Hydrological cycle* 2 (2009): 48.

De Jager, J., Geluk, M. C., Wong, T. E., Batjes, D. A. J., & de Jager, J. (2007). Geology of the Netherlands. *Petroleum Geology. Royal Netherlands Academy of Arts and Sciences, Amsterdam, The Netherlands*, *241*, 264.

Geluk, M. (1999). Late Permian (Zechstein) rifting in the Netherlands; models and implications for petroleum geology. *Petroleum Geoscience*, *5*(2), 189-199.

Geluk, M. C. (2000). Late Permian (Zechstein) carbonate-facies maps, the Netherlands. *Netherlands Journal of Geosciences*, *79*(1), 17-27.

Geluk, M. (Marinus C. (2005). *Stratigraphy and tectonics of Permo-Triassic basins in the Netherlands and surrounding areas*. s.n.].

Hay, W. W., Migdisov, A., Balukhovsky, A. N., Wold, C. N., Flögel, S., & Söding, E. (2006). Evaporites and the salinity of the ocean during the Phanerozoic: Implications for climate, ocean circulation and life. *Palaeogeography, Palaeoclimatology, Palaeoecology*, *240*(1–2), 3–46. https://doi.org/10.1016/j.palaeo.2006.03.044

Haq, B. U., & Schutter, S. R. (2008). A chronology of Paleozoic sea-level changes. *Science*, *322*(5898), 64-68.

Hirst, D. M., & Dunham, K. C. (1963). CHEMISTRY AND PETROGRAPHY OF THE MARL SLATE OF S. E. DURHAM, ENGLAND. In *Economic Geology* (Vol. 58). http://pubs.geoscienceworld.org/segweb/economicgeology/article-pdf/58/6/912/3481941/912.pdf

Jaworowski, K., & Mikołajewski, Z. (2007). Oil-and gas-bearing sediments of the Main Dolomite (Ca2) in the Międzychód region: a depositional model and the problem of the boundary between the second and third depositional sequences in the Polish Zechstein Basin. *Przegląd Geologiczny*, *55*(12/1), 1017-1024.

Kaiser, R., Nöth, S., & Ricken, W. (2003). Sequence stratigraphy with emphasis on platform-related parasequences of the Zechstein 2 carbonate (Ca2) - The northern platform margin of the Southern Permian Basin (NE Germany). *International Journal of Earth Sciences*, *92*(1), 54–67. https://doi.org/10.1007/s00531-002-0292-9

Lacombe, H., & Richez, C. (1982). The regime of the Strait of Gibraltar. In *Elsevier oceanography series* (Vol. 34, pp. 13-73). Elsevier.

Leeder, M. R., & Leeder, M. R. (2011). *Sedimentology and Sedimentary Basins : From Turbulence to Tectonics*. John Wiley & Sons, Incorporated. http://ebookcentral.proquest.com/lib/uunl/detail.action?docID=644991

Legler, B., Gebhardt, U., & Schneider, J. W. (2005). Late Permian non-marine–marine transitional profiles in the central Southern Permian Basin, northern Germany. *International Journal of Earth Sciences*, *94*(5), 851-862.

Manzi, V., Gennari, R., Lugli, S., Roveri, M., Scafetta, N., & Schreiber, B. C. (2012). High-frequency cyclicity in the mediterranean Messinian evaporites: Evidence for solar-lunar climate forcing. *Journal of Sedimentary Research*, *82*(12), 991–1005. https://doi.org/10.2110/jsr.2012.81

Mawson, M., & Tucker, M. (2009). High-frequency cyclicity (Milankovitch and millennial-scale) in slope-apron carbonates: Zechstein (Upper Permian), North-east England. *Sedimentology*, *56*(6), 1905–1936. https://doi.org/10.1111/j.1365-3091.2009.01062.x

Meijer, P. T., Slingerland, R., & Wortel, M. J. R. (2004). Tectonic control on past circulation of the Mediterranean Sea: A model study of the Late Miocene. *Paleoceanography*, *19*(1). https://doi.org/10.1029/2003PA000956

Meijer, P. T. (2006). A box model of the blocked-outflow scenario for the Messinian Salinity Crisis. *Earth and Planetary Science Letters*, *248*(1–2), 486–494. https://doi.org/10.1016/j.epsl.2006.06.013

Menning, M., Gast, R., Hagdorn, H., Käding, K. C., Simon, T., Szurlies, M., & Nitsch, E. (2005). Zeitskala für Perm und Trias in der Stratigraphischen Tabelle von Deutschland 2002, zyklostratigraphische Kalibrierung der höheren Dyas und Germanischen Trias und das Alter der Stufen Roadium bis Rhaetium 2005. *Newsletters on Stratigraphy*, *41*(3), 173–210. https://doi.org/10.1127/0078-0421/2005/0041-0173

Peryt, T.M., Geluk, M.C., Mathiesen, A., Paul, J. & Smith, K., (2010). Zechstein. In: Doornenbal, J.C. and Stevenson, A.G. (editors): Petroleum Geological Atlas of the Southern Permian Basin Area. EAGE Publications b.v. (Houten): 123-147

Schneider, J. W., & Scholze, F. (2018). Late Pennsylvanian-Early Triassic conchostracan biostratigraphy: A preliminary approach. In *Geological Society Special Publication* (Vol. 450, Issue 1, pp. 365–386). Geological Society of London. https://doi.org/10.1144/SP450.6

TNO-GDN (2022). Zechstein Groep. In: Stratigrafische Nomenclator van Nederland, TNO – Geologische Dienst Nederland. Geraadpleegd op 03-05-2022 op http://www.dinoloket.nl/stratigrafische-nomenclator/zechstein-groep.

Topper, R. P. M., & Meijer, P. T. (2013). A modeling perspective on spatial and temporal variations in Messinian evaporite deposits. *Marine Geology*, *336*, 44–60. https://doi.org/10.1016/j.margeo.2012.11.009

Van den Belt, F. J. G., de Boer, P. L., 2007. A shallow-basin model for ‘saline giants’ based on isostasy-driven subsidence. In: Nichols, G., Williams, E., Paola, C. (Eds.), Sedimentary Processes, Environments and Basins. International Association of Sedimentologists Special Publication 38, 241–252.

Van Der Baan, D. (1990). Zechstein reservoirs in the Netherlands. *Geological Society, London, Special Publications*, *50*(1), 379-398.

Van Wees, J.-D., Stephenson, R. A., Ziegler, P. A., Bayer, U., Mccann, T., Dadlez, R., Gaupp, R., Narkiewicz, M., Bitzer, F., & Scheck, M. (n.d.). *On the origin of the Southern Permian Basin, Central Europe*.

Warren, J. K. (2016). *Evaporites: a geological compendium* (Second). Springer.

Watts, A.B. (2001) Isostasy and Flexure of the Lithosphere. Cambridge University Press, Cambridge, 458 pp.

6 Appendices

Table 6.1. Volumes of the Zechstein deposits calculated using maps from the Southern Permian Basin Atlas (Peryt et al., 2010) and well tops from the Netherlands

Cycle	Unit	Area (m²)	Minimum volume (m³)	Maximum volume (m³)	Average volume (m³)
Z1	Kupferschiefer	6.11E+11	2.57E+11	5.30E+12	8.75E+11
	Carbonate	6.52E+11	4.80E+12	1.33E+13	9.04E+12
	Anhydrite	6.52E+11	7.17E+12	7.96E+13	2.43E+13
	Halite	4.94E+11	2.37E+12	1.05E+13	5.59E+12
Z2	Carbonate	5.50E+11	7.28E+12	1.48E+13	1.11E+13
	Lower anhydrite	5.50E+11	1.27E+12	3.99E+13	7.55E+12
	Salt/halite	5.47E+11	3.09E+13	4.40E+14	1.47E+14
	Roof anhydrite	5.50E+11	5.34E+11	7.64E+12	1.90E+12
Z3	Grey salt clay	6.56E+11	3.39E+11	3.81E+12	1.32E+12
	Carbonate	6.56E+11	3.26E+12	1.04E+13	6.85E+12
	Anhydrite	6.56E+11	6.70E+12	7.26E+13	2.55E+13
	Salt/halite	5.45E+11	2.22E+13	3.16E+14	1.08E+14
Z4	Red salt clay	4.05E+11	4.33E+11	5.99E+12	1.92E+12
	Anhydrite	4.05E+11	3.35E+11	7.46E+12	2.78E+12
	Salt/halite	4.05E+11	9.19E+12	8.73E+13	2.73E+13
Z5	Claystone	2.40E+11	4.42E+10	2.34E+11	1.39E+11
	Halite	2.40E+11	2.68E+11	4.01E+11	3.35E+11

Table 6.2. Comparison of the Z1-Z3 carbonate volumes calculated using the well tops from the Netherlands and the maps from the Southern Permian Basin Atlas (Peryt et al., 2010).

	Volume based on		
Z1 Carbonate	Well tops from the Netherlands	Maps from the SPBA	Difference
Minimum (m³)	1.70E+12	3.26E+12	-47.73%
Maximum (m³)	2.33E+13	1.04E+13	122.68%
Average (m³)	7.29E+12	6.85E+12	6.38%
Z2 Carbonate			
Minimum (m³)	2.06E+12	3.26E+12	-36.67%
Maximum (m³)	4.13E+13	1.04E+13	295.56%
Average (m³)	7.39E+12	6.85E+12	7.79%
Z3 Carbonate			
Minimum (m³)	2.09E+12	3.26E+12	-35.88%
Maximum (m³)	3.92E+13	1.04E+13	275.60%
Average (m³)	7.42E+12	6.85E+12	8.25%

Table 6.3. Volumes of water necessary for deposition the Zechstein sediments for water with the concentration at saturation.

		Mass (kg)			Volume of water necessary for deposition (m^3)			Average water depth (m)		
Cycle	Unit	Minimum	Maximum	Average	Minimum	Maximum	Average	Minimum	Maximum	Average
Z1	Carbonate	1.37E+16	3.78E+16	2.58E+16	9.54E+16	2.64E+17	1.80E+17	146427.72	405092.44	275760.08
	Gypsum	2.29E+16	2.54E+17	7.78E+16	4.37E+15	4.84E+16	1.48E+16	6699.25	74324.73	22737.22
	Halite	5.21E+15	2.31E+16	1.23E+16	1.92E+13	8.51E+13	4.53E+13	38.78	172.30	91.61
Z2	Carbonate	2.08E+16	4.23E+16	3.15E+16	1.45E+17	2.95E+17	2.20E+17	263308.54	536146.42	399727.48
	Gypsum	4.06E+15	1.27E+17	2.41E+16	7.73E+14	2.43E+16	4.59E+15	1404.54	44106.88	8352.66
	Halite	6.80E+16	9.67E+17	3.23E+17	2.50E+14	3.56E+15	1.19E+15	457.64	6512.16	2173.73
	Gypsum	1.71E+15	2.44E+16	6.09E+15	2.68E+14	4.65E+15	1.16E+15	487.14	8449.59	2105.92
Z3	Carbonate	9.28E+15	2.98E+16	1.95E+16	6.47E+16	2.08E+17	1.36E+17	98703.97	316845.87	207774.92
	Gypsum	2.14E+16	2.32E+17	8.15E+16	4.07E+15	4.42E+16	1.55E+16	6212.50	67336.04	23654.47
	Halite	4.89E+16	6.96E+17	2.37E+17	1.80E+14	2.56E+15	8.73E+14	329.79	4699.26	1600.50
Z4	Gypsum	1.07E+15	2.38E+16	8.90E+15	2.04E+14	4.54E+15	1.69E+15	503.71	11213.55	4186.39
	Halite	2.02E+16	1.92E+17	6.01E+16	7.44E+13	7.07E+14	2.21E+14	183.88	1748.04	546.72
Z5	Halite	5.91E+14	8.82E+14	7.37E+14	2.17E+12	3.25E+12	2.71E+12	9.06	13.54	11.30

Table 6.4. Minimum duration of deposition of the different Zechstein sediments with an assumed evaporation rate of 2 m/yr. The durations are calculated for the minimum, maximum and average volumes of deposits.

	Duration of deposition for an assumed evaporation rate of 2 m/yr (yr)											
	For the minimum volume				For the maximum volume				For the average volume			
Cycle	Carbonate	Gypsum	Halite	Total	Carbonate	Gypsum	Halite	Total	Carbonate	Gypsum	Halite	Total
Z1	56516	11603	162	6.83E+04	156351	128728	720	2.86E+05	106434	39380	383	1.46E+05
Z2	101628	3276	1913	1.07E+05	206934	91026	27225	3.25E+05	154281	18114	9088	1.81E+05
Z3	38096	10760	1379	5.02E+04	122291	116624	19646	2.59E+05	80194	40969	6691	1.28E+05
Z4		872	769	1.64E+03		19421	7308	2.67E+04		7251	2286	9.54E+03
Z5			38	3.79E+01			57	5.66E+01			47	4.72E+01
Total	1.96E+05	2.65E+04	4.26E+03	2.27E+05	4.86E+05	3.56E+05	5.50E+04	8.96E+05	3.41E+05	1.06E+05	1.85E+04	4.65E+05

Table 6.5. Fluxes of water into the basin in m3/yr

Cycle	Carbonate & gypsum	Halite
Z1	1.30E+12	9.88E+11
Z2	1.10E+12	1.09E+12
Z3	1.31E+12	1.09E+12
Z4	8.09E+11	8.09E+11
Z5		4.80E+11

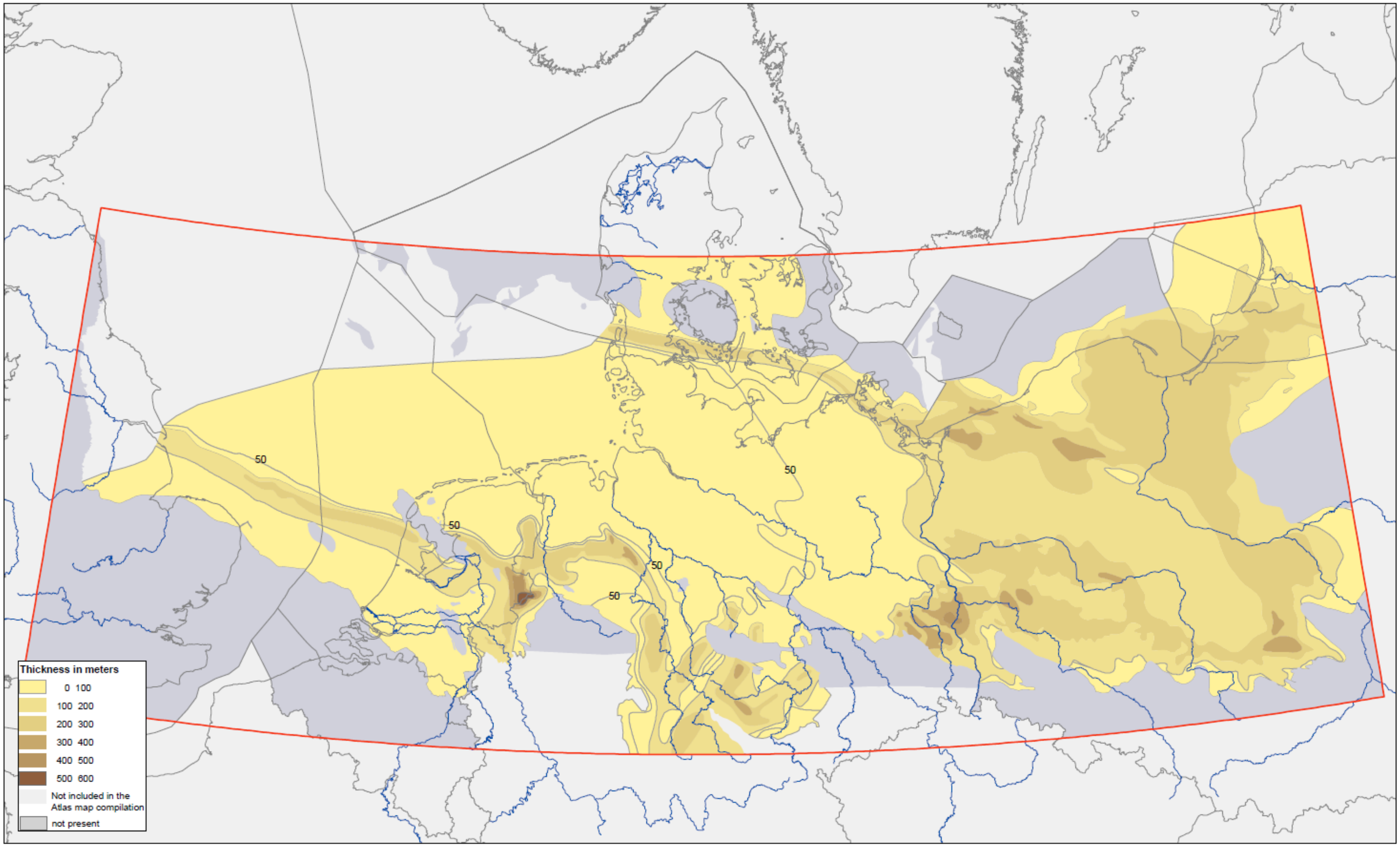

Figure 6.1. Distribution and thickness of the Z1 cycle, from Peryt et al. (2010).

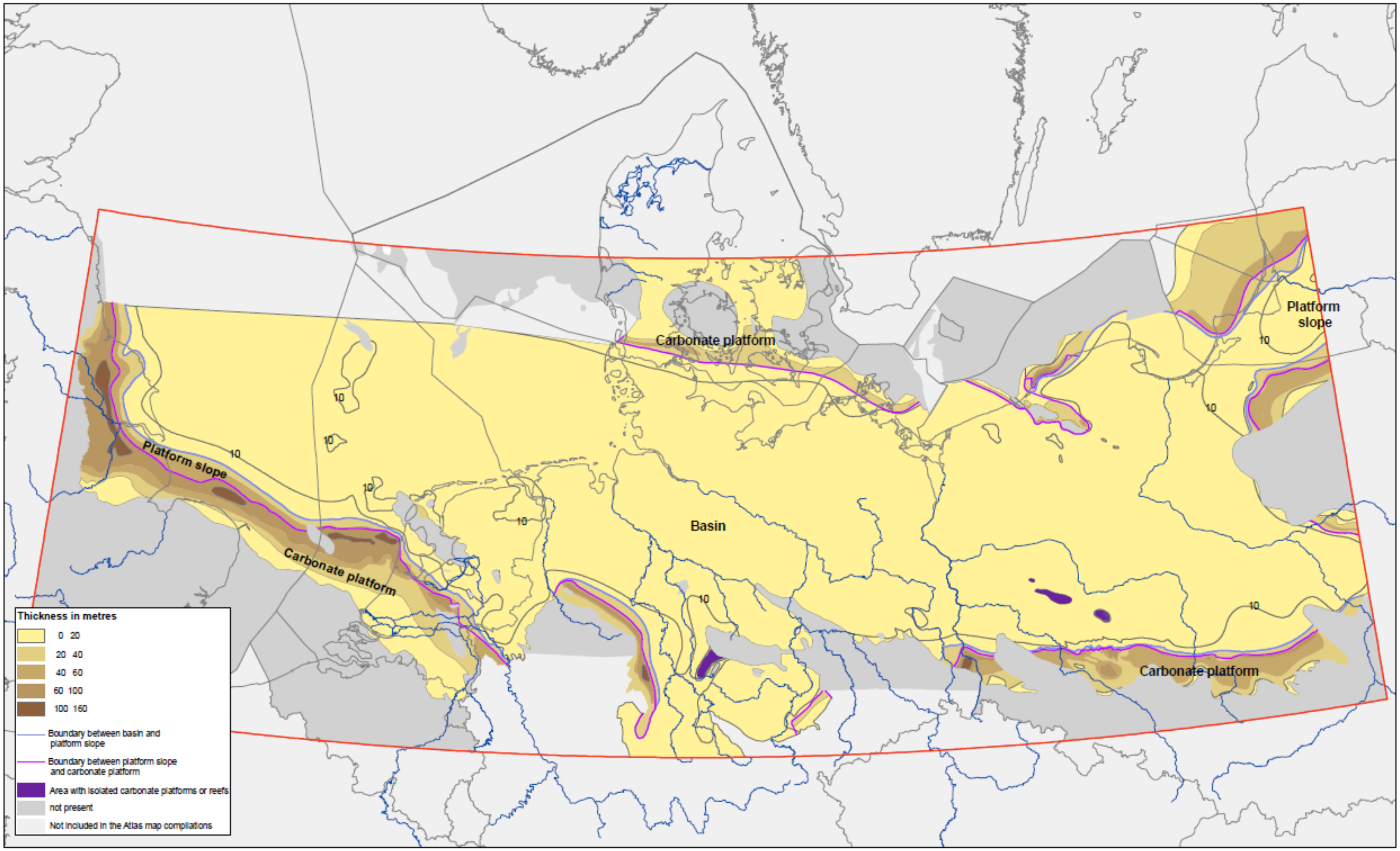

Figure 6.2. Distribution and thickness of the Z1 Carbonate, from Peryt et al. (2010).

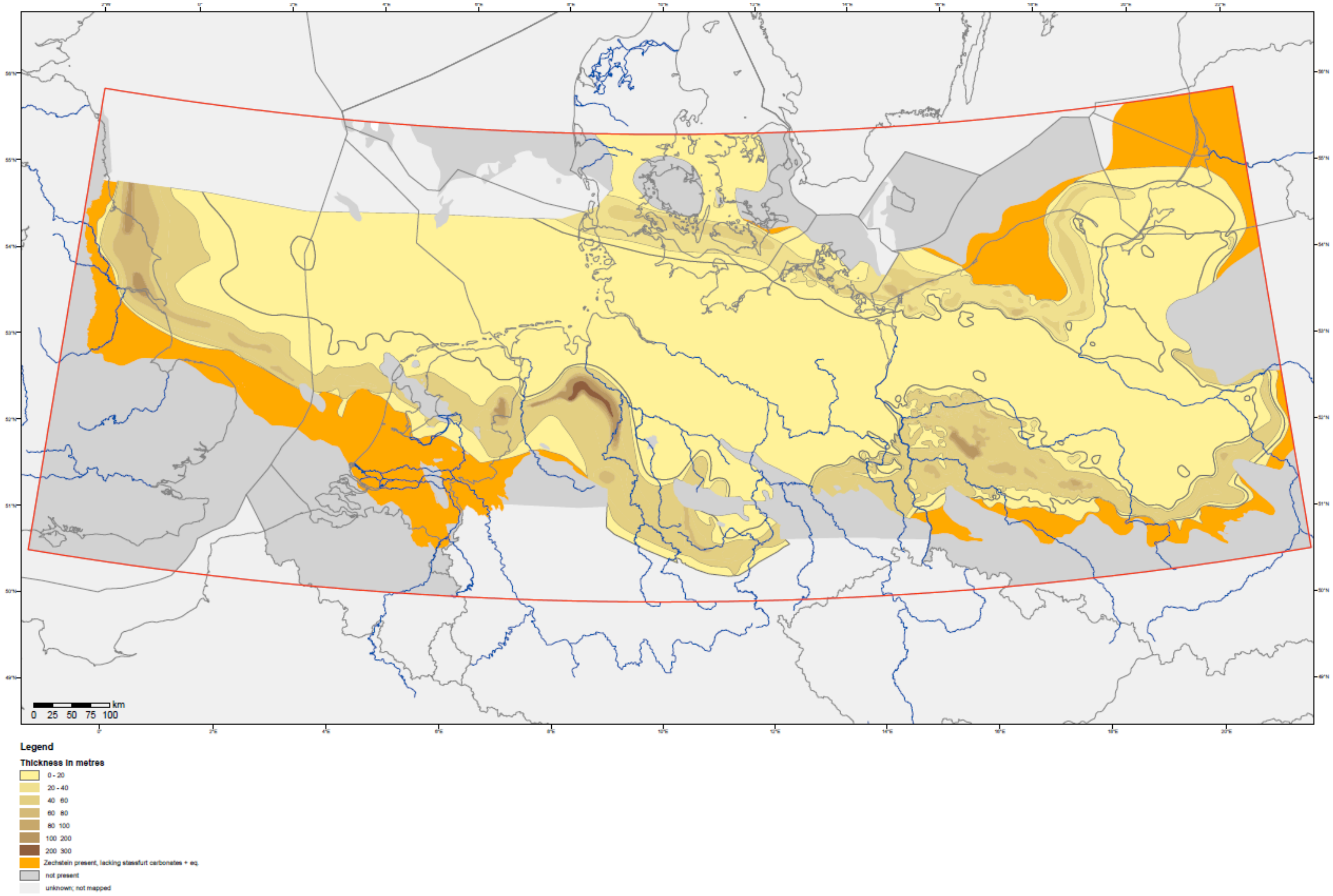

Figure 6.3. Distribution and thickness of the Z2 Carbonate, from Peryt et al. (2010).

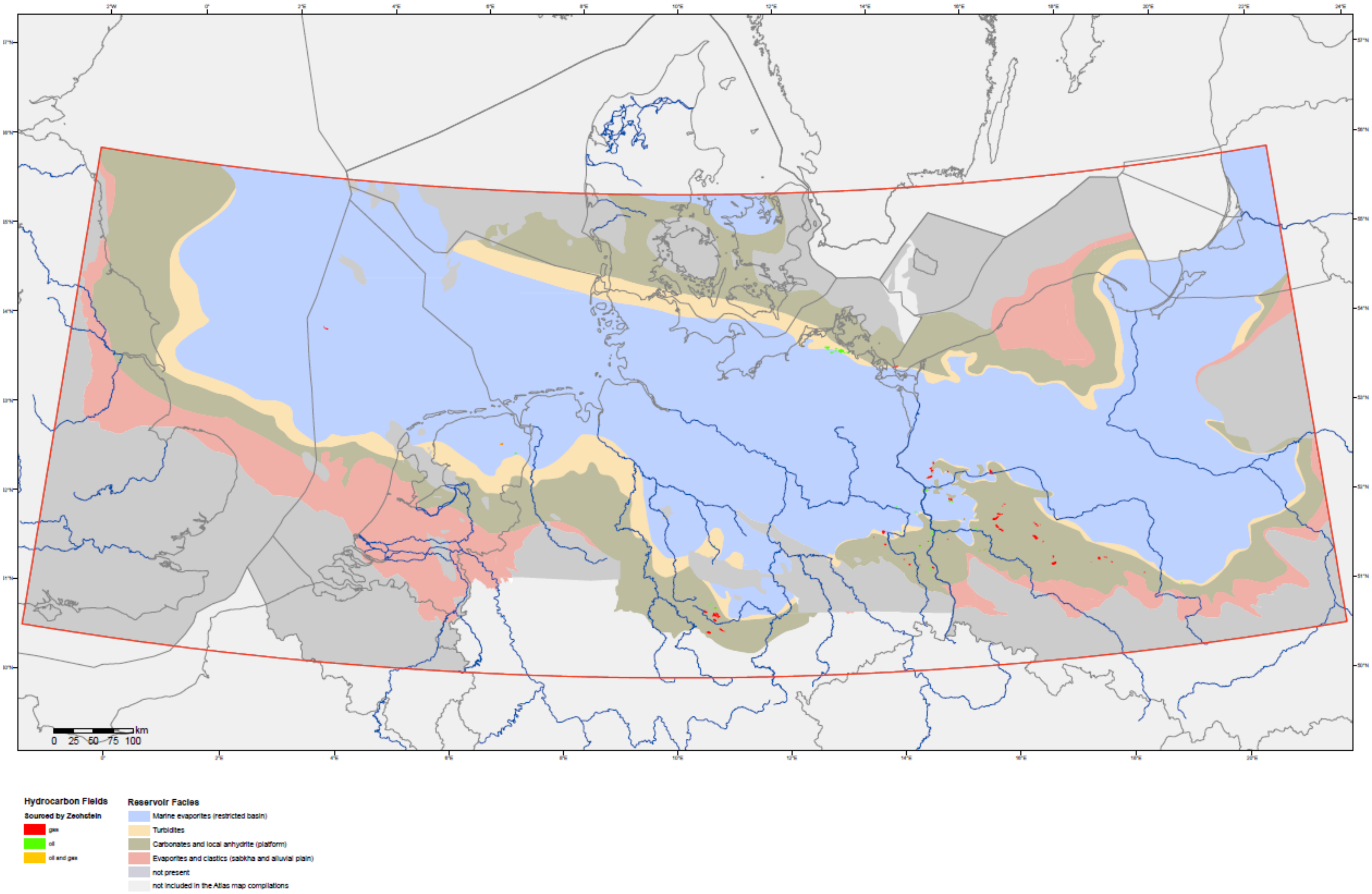

Figure 6.4. Distribution of the Z2 Carbonate facies, from Peryt et al. (2010).

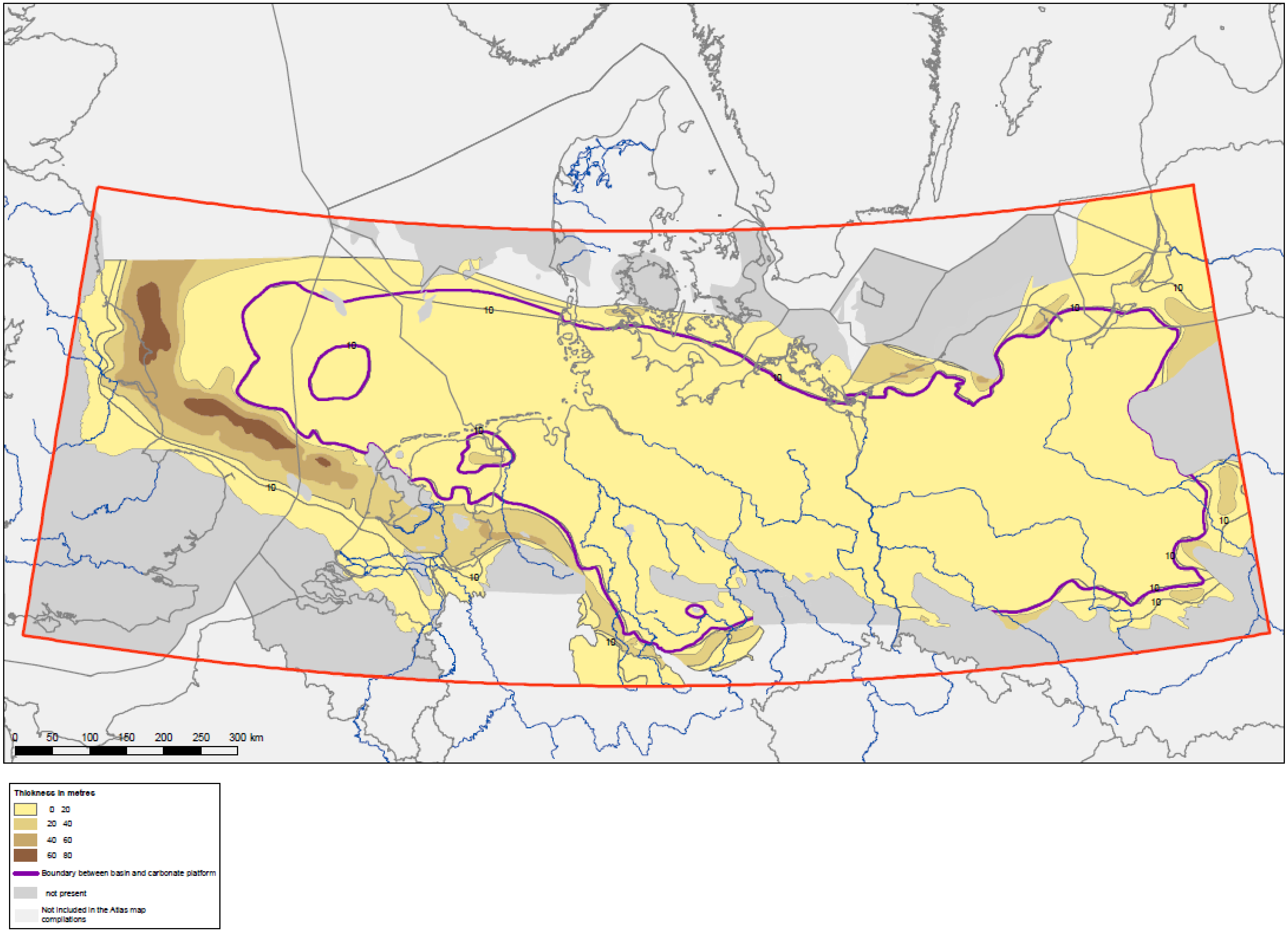

Figure 6.5. Distribution and thickness of the Z3 Carbonate, from Peryt et al. (2010).

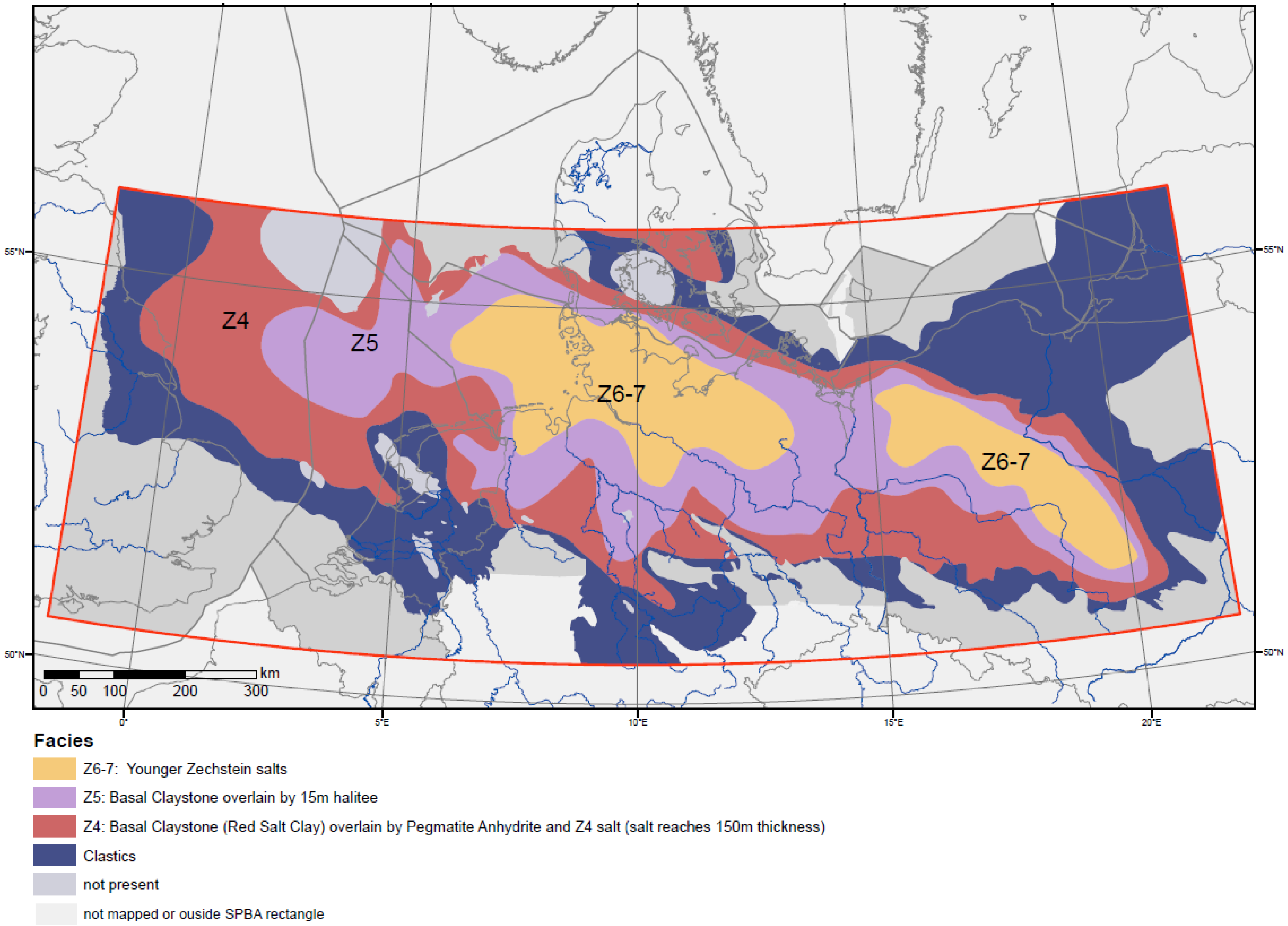

Figure 6.6. Distribution of the Z4-Z7 Zechstein sediments, from Peryt et al. (2010).

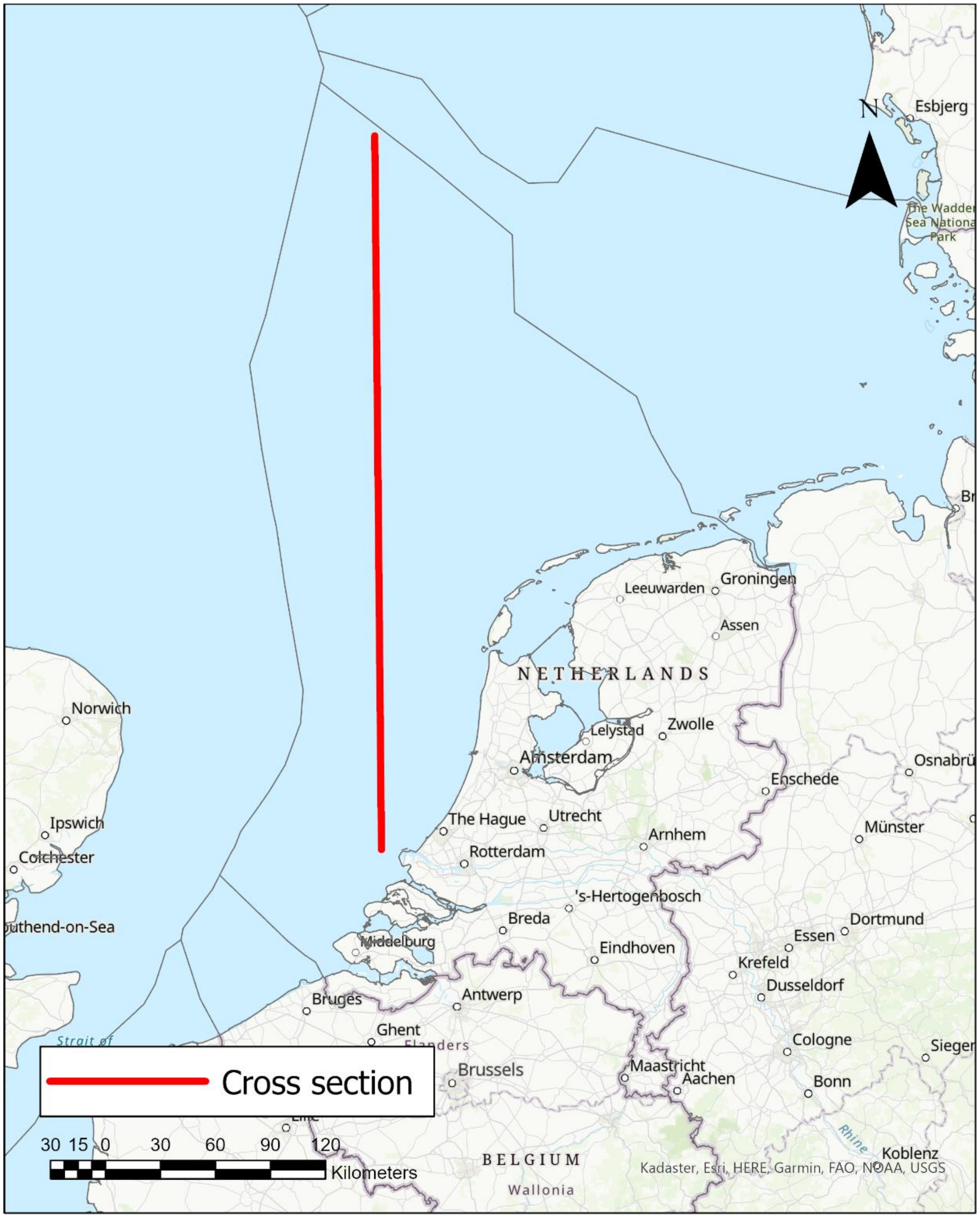

Figure 6.7. Location of the cross section.

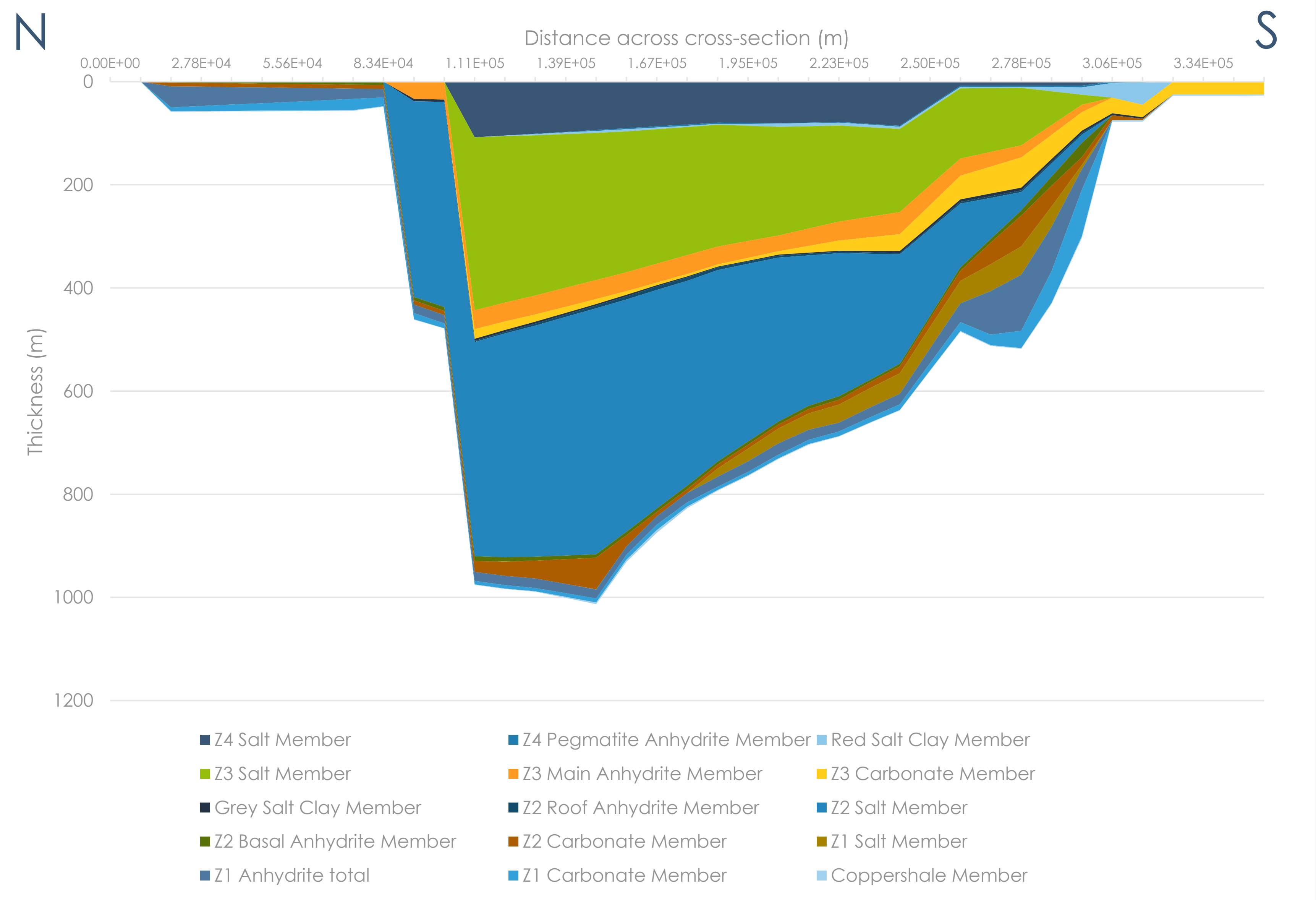

Figure 6.9. Cross-section, see Figure 6.8 for the location of the cross section. Data can be found in Table 6.6.

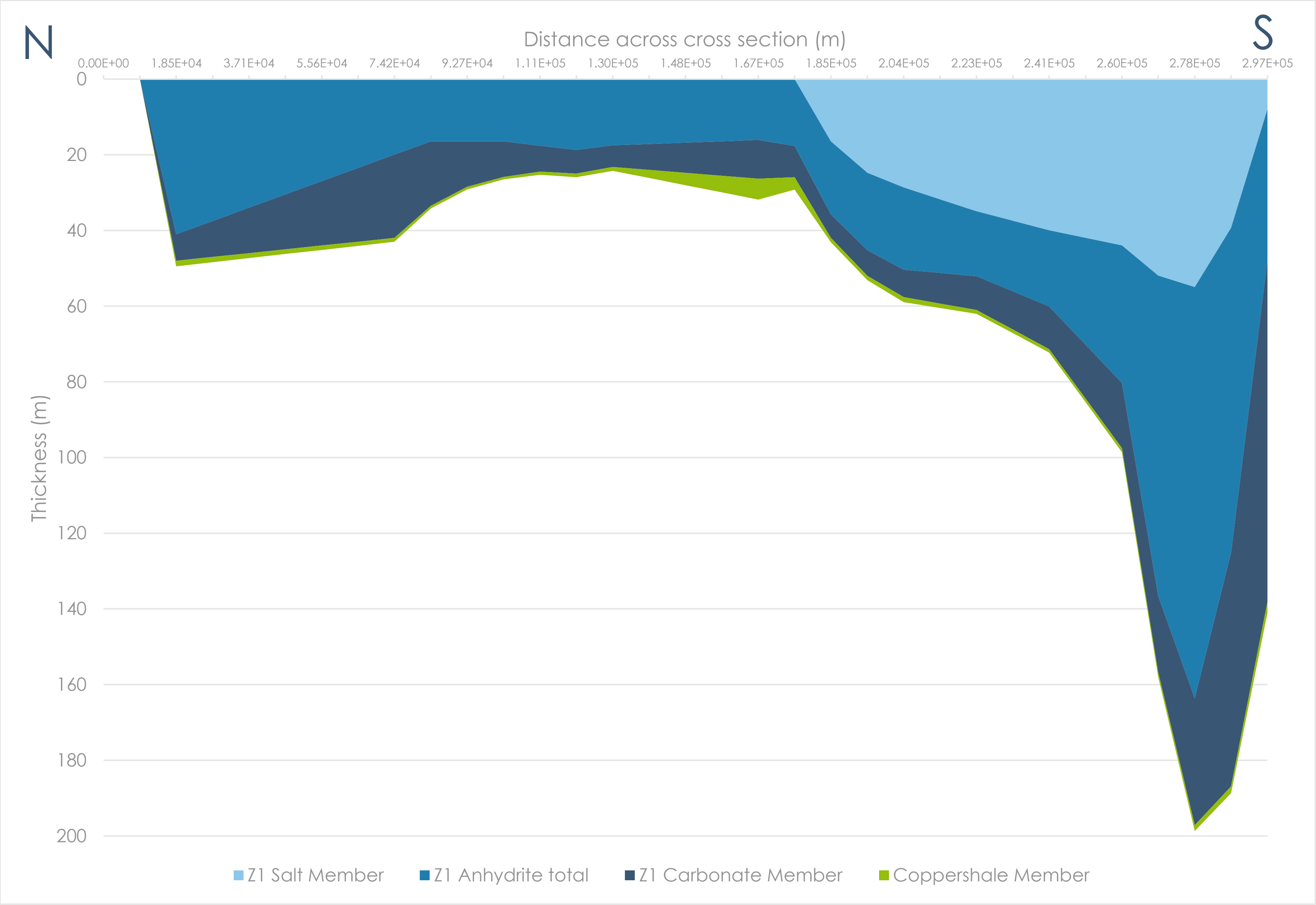

Figure 6.11. The Z1 part of the cross-section, as seen in Figure 6.10. Data can be found in Table 6.6..

Table 6.6. Thickness of all the Zechstein units in the Dutch subsurface across the cross section as given in Figure 6.10. Most left values are in the north and most right values are in the south.

	Length of cross section (m)										
	0.00	9271.77	18543.54	27815.30	37087.07	46358.84	55630.61	64902.38	74174.14	83445.91	92717.68
Zechstein unit	*Thickness of the unit (m)*										
Coppershale			1.50	1.42	1.33	1.25	1.17	1.08	1.00	0.75	0.71
Z1 Carbonate			7.00	9.50	12.00	14.50	17.00	19.50	22.00	16.98	11.96
Z1 Anhydrite total			40.98	37.48	33.98	30.47	26.97	23.47	19.97	16.46	16.46
Z1 Salt											
Z2 Carbonate			7.00	7.12	7.24	7.36	7.49	7.61	7.73	7.85	7.97
Z2 Basal Anhydrite			2.00	2.62	3.25	3.87	4.49	5.11	5.74	6.36	6.98
Z2 Salt											379.34
Z2 Roof Anhydrite											
Grey Salt Clay											4.50
Z3 Carbonate											
Z3 Main Anhydrite											33.48
Z3 Salt											
Red Salt Clay											
Z4 Pegmatite Anhydrite											
Z4 Salt											

Table 6.6. (continued)

	Length of cross section (m)									
	101989.45	111261.22	120532.98	129804.75	139076.52	148348.29	157620.06	166891.82	176163.59	185435.36
Zechstein unit	*Thickness of the unit (m)*									
Coppershale	0.67	0.83	0.88	0.93	2.14	3.26	4.38	5.50	3.30	1.11
Z1 Carbonate	9.39	6.83	6.55	6.26	6.84	7.97	9.11	10.25	8.21	6.18
Z1 Anhydrite total	16.45	17.59	18.16	18.73	18.12	17.51	16.44	16.09	17.70	19.31
Z1 Salt										16.50
Z2 Carbonate	7.65	20.99	27.66	34.33	47.83	61.34	21.71	8.50	7.91	7.33
Z2 Basal Anhydrite	7.98	8.98	8.41	7.84	7.27	6.70	6.62	6.60	6.28	5.96
Z2 Salt	397.51	415.68	433.85	448.25	462.66	477.06	450.60	424.14	397.69	371.23
Z2 Roof Anhydrite		1.99	2.65	3.76	4.45	5.13	5.82	6.50	6.27	5.24
Grey Salt Clay	4.28	4.05	3.83	3.60	3.38	3.15	2.93	2.70	1.97	1.25
Z3 Carbonate		18.89	16.56	14.23	11.90	9.56	7.23	4.90	4.68	4.46
Z3 Main Anhydrite	34.98	36.49	36.54	36.59	36.65	36.70	36.75	36.81	36.86	34.65
Z3 Salt		335.39	322.94	310.50	298.05	285.61	273.16	260.72	248.27	235.82
Red Salt Clay			1.32	2.65	3.08	3.51	3.94	3.26	2.57	1.89
Z4 Pegmatite Anhydrite				0.66	1.33	1.99	2.22	2.30	2.38	2.45
Z4 Salt		107.88	104.34	100.79	97.25	93.70	90.16	86.61	83.07	79.52

Table 6.6. (continued)

	Length of cross section (m)									
	194707.13	203978.90	213250.66	222522.43	231794.20	241065.97	250337.74	259609.50	268881.27	278153.04
Zechstein unit	*Thickness of the unit (m)*									
Coppershale	1.21	1.31	1.16	1.02	0.95	0.88	0.97	1.06	1.30	1.53
Z1 Carbonate	6.70	7.23	8.06	8.89	10.08	11.27	14.23	17.18	20.13	33.41
Z1 Anhydrite total	20.52	21.73	19.45	17.17	18.68	20.18	28.29	36.41	84.66	108.79
Z1 Salt	24.74	28.66	31.79	34.92	37.42	39.93	41.93	43.93	51.95	54.95
Z2 Carbonate	7.52	7.71	8.77	9.83	11.56	13.30	16.23	19.16	41.99	59.82
Z2 Basal Anhydrite	5.86	5.76	6.06	6.36	4.90	5.02	5.14	6.83	7.16	9.85
Z2 Salt	344.77	318.31	291.85	277.66	245.03	212.41	168.16	123.91	79.66	35.41
Z2 Roof Anhydrite	4.55	3.86	3.17	2.48	2.36	2.25	2.59	2.94	3.29	3.64
Grey Salt Clay	1.37	1.50	1.81	2.13	3.00	3.87	4.89	5.02	5.16	5.06
Z3 Carbonate	5.73	7.00	13.44	19.89	26.34	32.79	39.24	45.69	52.14	58.59
Z3 Main Anhydrite	32.44	30.23	33.43	36.64	39.85	43.06	38.21	33.36	28.52	23.67
Z3 Salt	223.38	210.93	198.49	186.04	173.60	161.15	148.70	136.26	123.81	111.37
Red Salt Clay	4.04	6.19	6.13	6.07	4.99	3.92	3.43	2.95	2.47	1.99
Z4 Pegmatite Anhydrite	1.73	1.00	1.11	1.22	1.66	2.10	2.07	2.05	2.02	1.99
Z4 Salt	79.94	80.37	79.17	77.97	81.76	85.56	46.73	7.89	7.92	7.94

Table 6.6. (continued)

	Length of cross section (m)							
	287424.81	296696.58	305968.35	315240.11	324511.88	333783.65	343055.42	352327.19
Zechstein unit	*Thickness of the unit (m)*							
Coppershale	1.77	2.88	2.97	3.06	2.76	2.46	2.15	1.85
Z1 Carbonate	61.78	90.15						
Z1 Anhydrite total	85.85	39.97						
Z1 Salt	39.29	7.98						
Z2 Carbonate	40.13	15.44	9.22	3.00				
Z2 Basal Anhydrite	17.46	27.44						
Z2 Salt	25.83	16.25						
Z2 Roof Anhydrite	3.30	2.96						
Grey Salt Clay	4.95	4.45	3.94	2.40				
Z3 Carbonate	47.42	36.26	30.40	24.55	24.66	24.76	24.87	24.97
Z3 Main Anhydrite	18.82	13.97						
Z3 Salt	65.54	19.71						
Red Salt Clay	8.04	14.10	28.53	42.97				
Z4 Pegmatite Anhydrite	2.51	3.02	2.35	1.68				
Z4 Salt	7.97	7.99						

Table 6.7. Thickness of the Z1 units in the three pseudo-wells in Figure 3.5 per timestep.

		Thickness per timestep (m)		
Zechstein unit	Timestep (yr)	Well 1	Well 2	Well 3
Coppershale Member	17000	5.50	1.02	1.53
Z1 Carbonate Member	123434	15.74	9.91	34.94
Z1 Anhydrite total	162814	31.83	27.08	143.73
Z1 Salt Member	163197	31.83	62.00	198.67

Table 6.8. Thickness of the Z1 units in the three pseudo-wells in Figure 3.5 per timestep adjusted for the vertical response as predicted by the isostatic balance for the carbonate, anhydrite and halite.

		Thickness per timestep (m)		
Zechstein unit	Timestep (yr)	Well 1	Well 2	Well 3
Coppershale Member	17000	5.50	1.02	1.53
Z1 Carbonate Member	123434	15.74	9.91	34.94
Z1 Anhydrite total	162814	20.93	15.45	70.03
Z1 Salt Member	163197	20.93	32.08	96.20

6.1 Python script

```
import numpy as np
import matplotlib.pyplot as plt

yr2sec = 365.25*24*3600
So = 41.86 # total salt concentration in Permian seawater
c = 145  # concentration at saturation of gypsum
rho = 2300        # gypsum, kg/m3
A = 6.5e11        # m2, roughly from Table 6.1
e = np.linspace( 0.1, 3, 30)

d = e*So/rho
plt.plot(e, d*1e3, label='Qb = 0')

for i in range(0, e.size):
    d[i] = e[i]*So/rho - (0.1*e[i]*(c-So))/rho
    if d[i] < 0:
        d[i] = np.nan

plt.plot(e, d*1e3, label='Qb = 0.1*e*A')

for i in range(0, e.size):
    d[i] = e[i]*So/rho - (0.2*e[i]*(c-So))/rho
    if d[i] < 0:
        d[i] = np.nan

plt.plot(e, d*1e3, label='Qb = 0.2*e*A')

for i in range(0, e.size):
    d[i] = e[i]*So/rho - (0.3*e[i]*(c-So))/rho
    if d[i] < 0:
        d[i] = np.nan

plt.plot(e, d*1e3, label='Qb = 0.3*e*A')

for i in range(0, e.size):
    d[i] = e[i]*So/rho - (0.4*e[i]*(c-So))/rho
    if d[i] < 0:
        d[i] = np.nan

plt.plot(e, d*1e3, label='Qb = 0.4*e*A')

plt.xlabel('Rate of Net Evaporation [m/yr]')
plt.ylabel('Rate of Deposition [mm/yr]')
plt.grid(True)
plt.legend()
plt.show()
```